



UNIVERSITY OF INDONESIA

TITLE

**RESERVOIR CHARACTERIZATION USING AVO ANALYSIS AND SIMULTANEOUS
INVERSION, CASE STUDY AT NSH FIELD, EAST JAVA**

THESIS

NAME : FEBY SYOFIA HAPSARI
NPM : 0706171913

FACULTY OF MATHEMATICS AND NATURAL SCIENCES
PROGRAM STUDY OF PHYSICS SCIENCES
JAKARTA
MAY 2010



UNIVERSITY OF INDONESIA

TITLE

**RESERVOIR CHARACTERIZATION USING AVO ANALYSIS AND SIMULTANEOUS
INVERSION, CASE STUDY AT NSH FIELD, EAST JAVA**

THESIS

Submitted as parts of requirements to achieve the Master Degree

NAME : FEBY SYOFIA HAPSARI
NPM : 0706171913

FACULTY OF MATHEMATICS AND NATURAL SCIENCES
PROGRAM STUDY OF PHYSICS SCIENCE
JAKARTA
MAY 2010

PAGE OF ORIGINALITY

I hereby notify that this thesis is my original work, and all of the sources that has been cited or referred has been explained or stated clearly.

Name : Feby Syofia Hapsari

NPM : 0706171913

Date : 03 July 2010

Signature : 



PAGE OF APPROVAL

Thesis submitted by :
Name : Feby Syofia Hapsari
NPM : 0706171913
Program Study : Physics Graduate Program, Reservoir Geophysics
Title : Reservoir Characterization using AVO Analysis and
Simultaneous Inversion, Case Study NSH Field, East Java

Has been succeeded to defend in front of the committee member and accepted as part of requirement to achieve the Master degree at Reservoir Geophysics, Physics Graduate Program, Faculty of Mathematics and Natural Sciences, University of Indonesia.

Committee Member

Counselor 1 : Prof. Dr. Suprayitno Munadi (.....Signature.....)

Counselor 2 : (.....Signature.....)

Examiner 1 : Dr. Abdul Haris (.....Signature.....)

Examiner 2 : Dr. Waluyo (.....Signature.....)

Examiner 3 : Dr. Ricky Adi Wibowo (.....Signature.....)

Place : Jakarta

Date : July 03, 2010

ACKNOWLEDGEMENTS

First, I would like to say thank you to Allah S.W.T. for the godsend that given to me, so by His help my thesis's finally done, even though the result was not perfect, but all effort already given to finish this thesis, and I would like say thank you to :

1. Erfan Taufik Hidayat and Falah Athaurrahman Hidayat, for the support.
2. Bapak Prof. Dr. Suprayitno Munadi for the mentoring and his guidance.
3. Bapak Dr. Yunus Daud and Dr. Abdul Haris as the Head and the Secretary from Reservoir Geophysics Post Graduate Program.
4. My parents, brother and sister.
5. All partner in the office at Humpson Russel.
6. Bapak Samiji and Suparman that helped in the administration things.
7. All lecturers and the assistant at Reservoir Geophysics Post Graduate.
8. All colleagues at Reservoir Geophysics Post Graduate Program.

Jakarta, May 2010

Feby Syofia Hapsari

**PAGE OF THESIS PUBLICATION AGREEMENT
FOR ACADEMIC INTEREST**

As a student of University of Indonesia, I am :

Name : Feby Syofia Hapsari
NPM : 0706171913.....
Program : Physical Science.....
Department : Reservoir Geophysics
Faculties : Mathematics and Natural Sciences
Type : Thesis

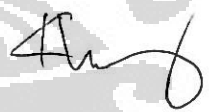
For the development in sciences, hereby I agree to giving the University of Indonesia the *Non-exclusive Royalty-Free Right* for my thesis result below:

Reservoir Characterization Using AVO Analysis and Simultaneous Inversion, Case Study at NSH Field, East Java

.....
with the hardware (if necessary). By this Non-exclusive Royalty-Free Right, University of Indonesia could to keep, change the format media, keep and publicity my thesis as long as putting my name as the writer and copyright owner.

Hereby I make this statement with honest.

Made in : Jakarta
Date : 03 July 2010.....


(Feby Syofia Hapsari)

ABSTRACT

Simultaneous Inversion is a method that used in the AVO inversion, that process the partial stacking as input and the elastic parameter and impedances as output in one batch.

Lambda Mu Rho is a method that used elastic parameter for the analysis: Lambda as the incompressibility parameter, the ability of rocks to transform their volume when are given a stress and Mu as the rigidity parameter, the ability of rocks to transform their shape when are given a stress.

This study was carried out in carbonate reservoir to present qualitative fluid classification with level of confidence based on Simultaneous seismic Inversion. Rock physics analysis was also conducted to quantitatively estimate Lambda Mu Parameter.

The final product of this study workflow is a 3D cube of reservoir characterization with uncertainties which consist of probability of wet carbonate and gas carbonate, and Lambda Mu Rho (Lambda-Rho and Mu-Rho 3D cube). As object of the study, the data from offshore East Java was used.

ABSTRAK

Metoda inversi simultan merupakan salah satu metoda yang digunakan dalam proses AVO inversion, yang didalam prosesnya mengolah input seismik 'partial stacking' dalam satu proses untuk menghasilkan volume seismik untuk parameter elastik dan impedansi.

Metoda Lambda Mu Rho merupakan metoda yang menggunakan parameter elastik dalam analisisnya, dimana Lambda merupakan parameter incompressibilitas, yaitu kemampuan batuan dalam terbentuknya perubahan volume apabila terkena *stress* dan Mu merupakan parameter *rigiditas* dari batuan, yaitu kemampuan batuan dalam perubahan bentuk apabila terkena *stress*.

Study ini mempelajari reservoir karbonat dengan memberikan analisa secara kualitatif untuk klasifikasi fluida dengan menggunakan inversi simultan. Analisa 'RockPhysics' dilakukan untuk mengestimasi secara kualitatif parameter-parameter dari Lambda Mu Rho.

Hasil akhir dari study ini adalah seismik 3D untuk karakterisasi reservoir dengan ketidakpastiannya yang terdiri dari reservoir karbonat dengan kandungan gas dan air, dan juga Lambda Mu Rho volume (Volume 3D untuk Lambda-Rho dan Mu-Rho). Objek penelitian yang digunakan adalah data dari offshore di Jawa Timur.

TABLE OF CONTENTS

	Page
Page of Originality	i
Page of Approval	ii
Acknowledgment	iii
Page of Thesis Publication Agreement for Academic Interest	iv
Abstract	v
Table of Contents.....	vi
Table of Figures	viii
Tables	xi
CHAPTER 1. Introduction	1
1.1. Background	1
1.2. Objective	1
1.3. Scope of Works	1
1.4. Area of Study	2
CHAPTER 2. Data and Methodology	4
2.1. Data Provided	4
2.2. Data Used	4
2.3. Methodology	4
CHAPTER 3. Basic Theory.....	7
3.1. Amplitude Variation with Offset	7
3.1.1. Basic Principle of AVO Method	7
3.1.2. Reflected Coefficient of Zero Incidence Angle	7
3.1.3. Poisson's Ratio	9
3.1.4. Simplification of Zoeppritz Equation	11
3.1.5. Gas Detection on Medium	13
3.1.6. AVO Attributes	14
3.2. Lambda-Mu-Rho (LMR) Attribute	15
3.2.1. Definition of LMR	15
3.2.2. Goodway Approximations	16

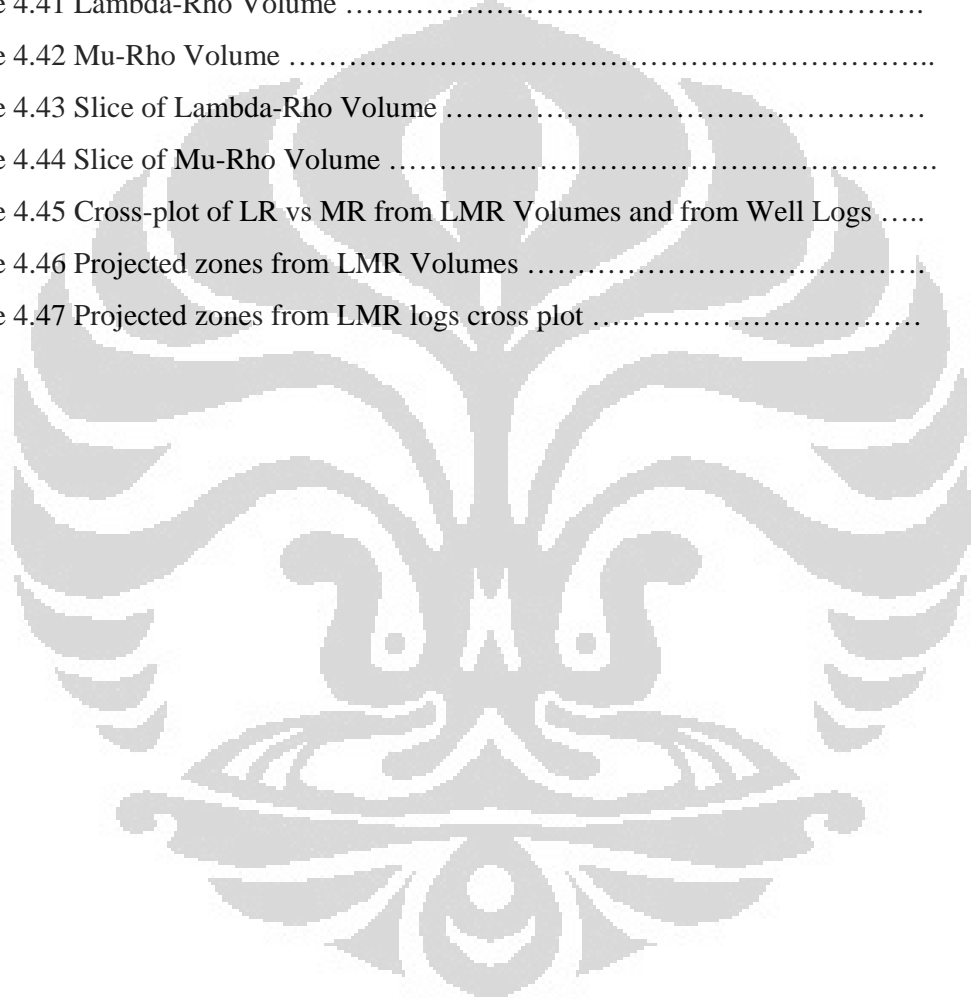
CHAPTER 4. Processed Data and Analysis	19
4.1. Log Property Cross-plots	19
4.1.1. Vp versus Vs	19
4.1.2. Zp versus VpVs Ratio	20
4.1.3. Vp versus Density	21
4.1.4. LMR Logs	22
4.2. Well Seismic Tie	23
4.2.1. Applying Check-shot correction	23
4.2.2. Statistical Well Correlation	24
4.2.3. Seismic Well Correlation	24
4.3. Seismic Data Loading and Conditioning	28
4.3.1. Loading NMO Corrected Gathers	28
4.3.2. Determining Seismic Polarity.....	29
4.3.3. Seismic Data Conditioning.....	29
4.4. AVO Analysis	34
4.4.1. AVO Attribute Extractions	35
4.5. Simultaneous Inversion	37
4.5.1. Initial Model Construction and Inversion Parameter Testing ...	38
4.5.2. Simultaneous Inversion	42
4.5.3. Interpretation and Cross-plotting	44
4.5.4. LMR: Interpretation and Cross-plotting	47
CHAPTER 6. Conclusion and Recommendations	53
References.....	54

TABLE OF FIGURE

	Page
Figure 1.1 Location of Area of Study (PE Internal Report)	2
Figure 1.2 East Java Basin Stratigraphy (PE Internal Report)	3
Figure 2.1 Flow chart for AVO analysis	5
Figure 2.2 Simultaneous inversion flow chart	6
Figure 3.1 relationship between offset and incidence angle	7
Figure 3.2 Reflected Coefficient of zero incidence angle.....	8
Figure 3.3. (a) normal polarity and reverse polarity for the minimum phase wavelet and (b) zero phase wavelet	9
Figure 3.4 A cylinder with the pressure at its top and bottom of cylinder	10
Figure 3.5 Poisson ratio value based on the medium (Wren,1984).....	10
Figure 3.6 Plot of P wave reflected coefficient versus incidence on the interface for Poisson ratio at 0.2 and 0.3 (a), depleted Poisson ratio (b)and Increased Poisson rat Plot koefisien refleksi gelombang P versus sudut datang pada interface untuk ratio (c) (Ostrander, 1984).....	11
Figure 3.7 Sand category based on AVO characteristic	14
Figure 3.8 Illustration of rocks matrix (a)normal condition, (b) compressed and (c)pressure shifted (Royle, 1999)	16
Figure 3.9 The comparison between crossplot of P impedance vs S impedance log and crossplot Lambdha-Rho vs Mu-Rho (Goodway et al, 1997)	18
Figure 4.1 NSH-1 Well Cross plot of Vp versus Vs, color coded by different petrophysical logs	19
Figure 4.2 NSH-1 Well Cross plot of Vp versus Vs showing zone that highlighted the HC anomaly.....	20
Figure 4.3 Well Cross plot of Zp versus Vp/Vs, color coded by different logs	20
Figure 4.4 NSH-1 Well Cross plot of Zp versus Vp/Vs showing zone that highlighted the HC anomal	21
Figure 4.5 NSH-1 Well Cross plot of Vp versus Density, color coded by different logs	21
Figure 4.6 NSH-1 Well Cross plot of LR versus MR, color coded by Water Saturation	22
Figure 4.7 NSH-1 Well Cross plot of LR versus MR, showing zone that highlighted the HC anomaly	22

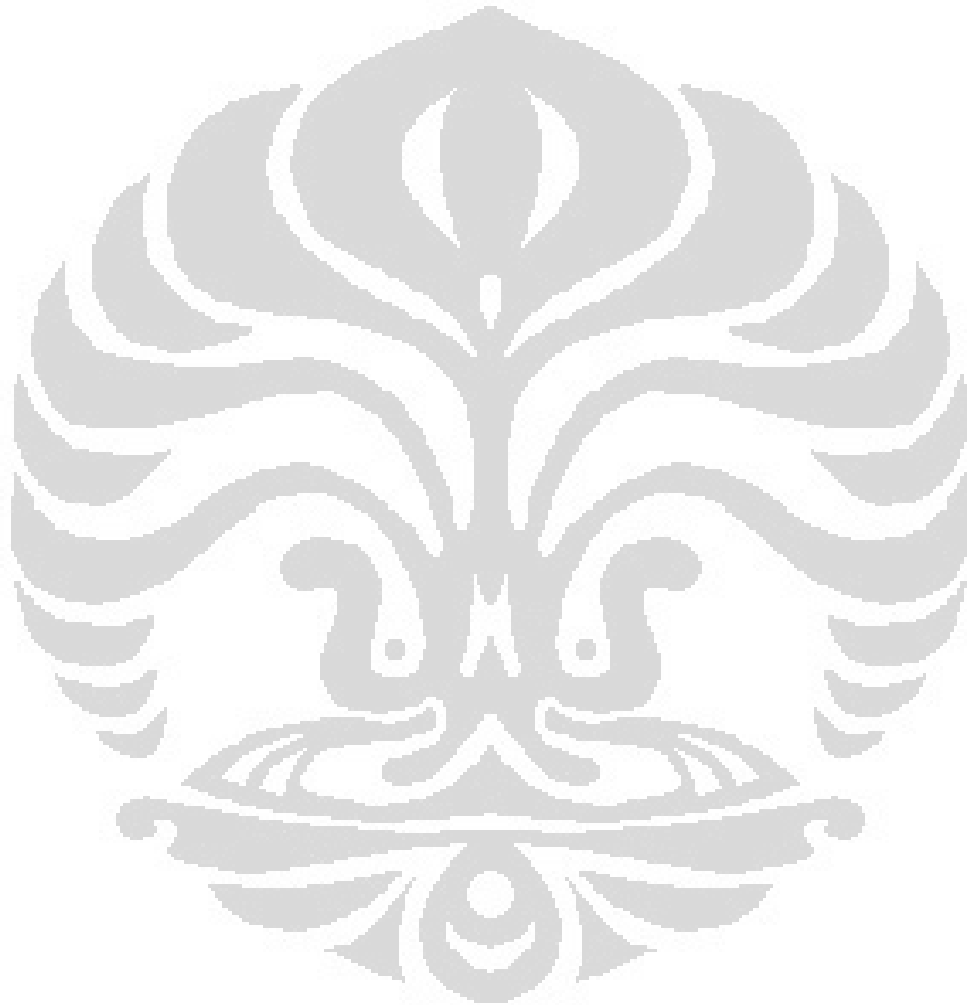
Figure 4.8 Displaying the check shot data	24
Figure 4.9 Statistical Wavelet used in the Well Correlation process	24
Figure 4.10 Initial correlation after check-shot correction was -11.4%. Notice that check-shot does not reach TD	25
Figure 4.11 Correlated on two strongest events: NGRAYONG and KUJUNG1. Applied stretch to time-depth curve	26
Figure 4.12 After fixing the NGRAYONG and KUJUNG 1 picks, correlated events below the check-shot log. Applied stretch	26
Figure 4.13 After slight +4 degree wavelet phase rotation, the final correlation is now 49% from NGRAYONG -100 ms o BASEMENT	27
Figure 4.14 NMO Corrected Gathers and the 3D Basemap showing fold	28
Figure 4.15 Determining the seismic polarity	29
Figure 4.16 NMO Corrected Gathers	30
Figure 4.17 Trace Mute	30
Figure 4.18 Super Gather	31
Figure 4.19 Bandpass Filter	31
Figure 4.20 Radon 1st pass	32
Figure 4.21 Radon 2nd pass	32
Figure 4.22 Trim Static	33
Figure 4.23 Angle Gather	33
Figure 4.24 Seismic Conditioning Parameters	34
Figure 4.25 AVO Analysis	35
Figure 4.26 AVO Attribute showing Gradient*sign (Intercept)	37
Figure 4.27 Initial Model of Zp, Zs and Density, built using NSH-1 Well logs	39
Figure 4.28 Initial Model of Zp, Zs and Density, built using NSH-1 Well logs and then merged with the RMS Velocity	40
Figure 4. 29 Inversion Parameter Testing (pre-stack Inversion Analysis)	41
Figure 4. 30 Zp volume	42
Figure 4. 31 Zs volume	42
Figure 4. 32 Dn volume	43
Figure 4.33 Vp/Vs ratio volume	43
Figure 4.34 Slice of Zp, showing Mean of P-Impedance from a 25 ms window below Kujung 1	44
Figure 4.35 Slice of Zs, showing Mean of S-Impedance from a 25 ms window below	

Kujung 1	45
Figure 4.36 Slice of Vp/Vs, showing Mean of Vp/Vs from a 25 ms window below Kujung 1	45
Figure 4.37 Cross-plot of AI vs VpVs from Inversion and from Well Logs	46
Figure 4.38 The projected zone from AI-VpVs from Inversion cross-plot	46
Figure 4.39 The projected zone from AI-VpVs from Well log cross-plot	47
Figure 3.40 Slice of the Cross plot zone	47
Figure 4.41 Lambda-Rho Volume	48
Figure 4.42 Mu-Rho Volume	48
Figure 4.43 Slice of Lambda-Rho Volume	49
Figure 4.44 Slice of Mu-Rho Volume	49
Figure 4.45 Cross-plot of LR vs MR from LMR Volumes and from Well Logs	50
Figure 4.46 Projected zones from LMR Volumes	51
Figure 4.47 Projected zones from LMR logs cross plot	51



TABLE

	Page
Tabel 3.1 Sensitivity analysis using Petrophysics (Goodway et al, 1997)	17



CHAPTER I

INTRODUCTION

1.1 Background

Future development of the NSH field reservoir requires the best possible information available in order to minimize risks and maximize reservoir production. Careful processing and interpretation of 3D seismic data has been a proven cost-effective method for delineating and characterizing reservoirs throughout the world and a geophysical study of the NSH 3D seismic.

Two interpretation approaches were applied in this study of the geophysical data for the NSH Field: AVO Analysis and Simultaneous Inversion. The belief is that these two technologies will provide better information to delineate the reservoir limits as well as map the reservoir characteristics.

1.2 Objective

The objective of this thesis project is to provide information to delineate the reservoir limit as well as to map the reservoir characteristics.

1.3 Scope of Works

The scope of works for this thesis project includes:

- LAS well log data loading to a new database to include tops depth-time and check shot
- Basic well log editing and petrophysical analysis to create a complete suite of well logs (Sonic, Density, Shear wave) over the define target interval in depth
- Load a complete set of SEG-Y format gathers, create geometry and insert well data
- Load a complete set of velocity information for offset-angle transform
- Seismic data conditioning over the target interval (Maximum 1 second)
- Well-seismic tie and synthetic generation

- Initial model construction and inversion parameter testing
- Simultaneous Inversion over a complete area
- Interpretation and cross-plotting (including LMR attributes)

1.4. Area of Study

In this thesis, the analysis was conducted in carbonate reservoir in NSH Field, in East Java Basin. This Field is approximately located 80 Km from Tuban city, and 160 Km from Surabaya (Figure 1.1.).



Figure 1.1 Location of Area of Study (PE Internal Report)

The exploration objective was to evaluate gas potential within Kujung carbonate build-up and Tuban Sandstones up-dip from the Kepodang Gas Field, and also oil potential in basal clastic which pinched out against basement. Specific for this study the focus is in gas analysis of Kujung Carbonate build-up. Figure 1.2, showing general stratigraphy of the East Java Basin.

Kujung carbonate in this study was divided into two zones, Kujung-I and Kujung-II. The reservoir might have been sourced from both the east and the west. From the analyses of previous wells, it was recovered that Kujung unit I and II contained gas with high CO₂. This CO₂ was analyzed to be generated from Muriah and Lasem volcanoes which intruded the Kujung shelf at approximately 1.0 MYBP. In addition, the reservoir in this might be sourced from the Bawean Trough to the East. Based upon maturity mapping, the Ngimbang Formation source rocks are currently within the oil window. During tectonic quiescence prior to the regional inversion event the preferred direction for migration was along the sediment-basement interface, updip to the west onto the paleo high. This potential Kujung reservoir was regionally sealed with the Tuban and Wonocolo (PE Internal Report,-).

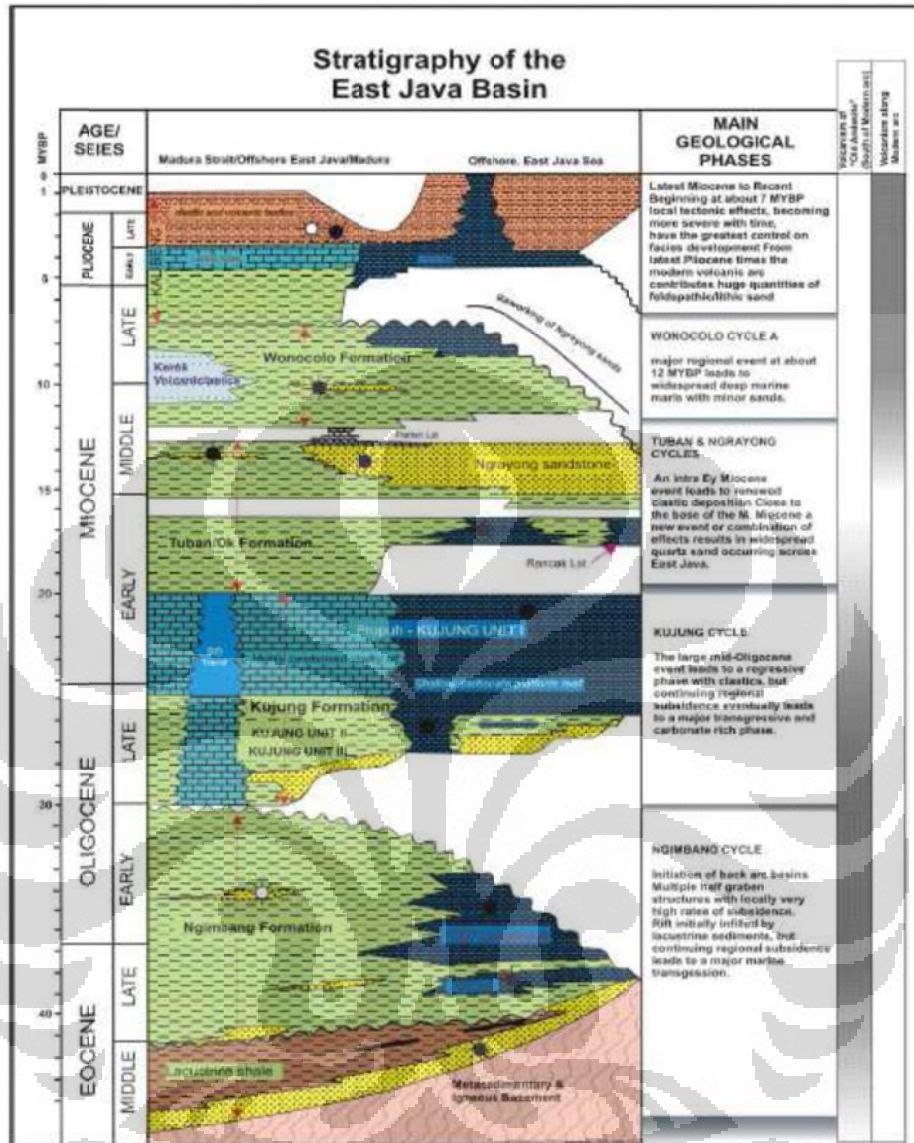


Figure 1.2 East Java Basin Stratigraphy (PE Internal Report)

In the newly acquired 3D seismic data, the time interpretation of Kujung-I event shows that Kujung-I is recognized as carbonate build up. There is a high zone in North East of survey which might be the perfect trap in the petroleum system.

CHAPTER 2

DATA AND METHODOLOGY

2.1. Data Provided

- Well : Received data for NSH-1 Well in numerous LAS files and well reports.
- Seismic : Received one NMO Corrected Gather in SEG-Y format.
- Horizons: Five horizons data
- RMS Velocity

2.2. Data Used

To support this study, following data was used in the area of study,

- 3D Angle Gather Seismic
- 3D Post Stack Seismic
- 1 well data was available, NSH-1, log data are gamma ray, caliper, deep resistivity, density, neutron porosity, compressional sonic log, shear sonic log, checkshot data, and also petrophysical log analysis (VClay, Water Saturation, and Porosity)

2.3. Methodology

The methodology to characterize the reservoir will be divided into two main parts. First, the AVO analysis, which has the objective to analyse the amplitude versus offset response on the seismic volume and the second part is the AVO inversion, with the objective to create LMR volume using simultaneous inversion

The flow chart of AVO analysis is summarized in figure 2.1, AVO analysis was done at the PSTM CDP gather. Before conducting the analysis, the seismic was processed to improve the signal to noise ratio by filtering, muting, scaling and NMO correction, then create the super gather and angle gather volume.

Figure 2.2 shows the flow chart for the simultaneous inversion, the input for this simultaneous inversion is P-wave, S-wave, Density log and the PSTM CDP gather volume, then the results consist of Acoustic Impedance, Shear Impedance, and Density. After the Simultaneous Inversion was done, then creates the Lambda-Rho and Mu-Rho volume from the impedance volume.

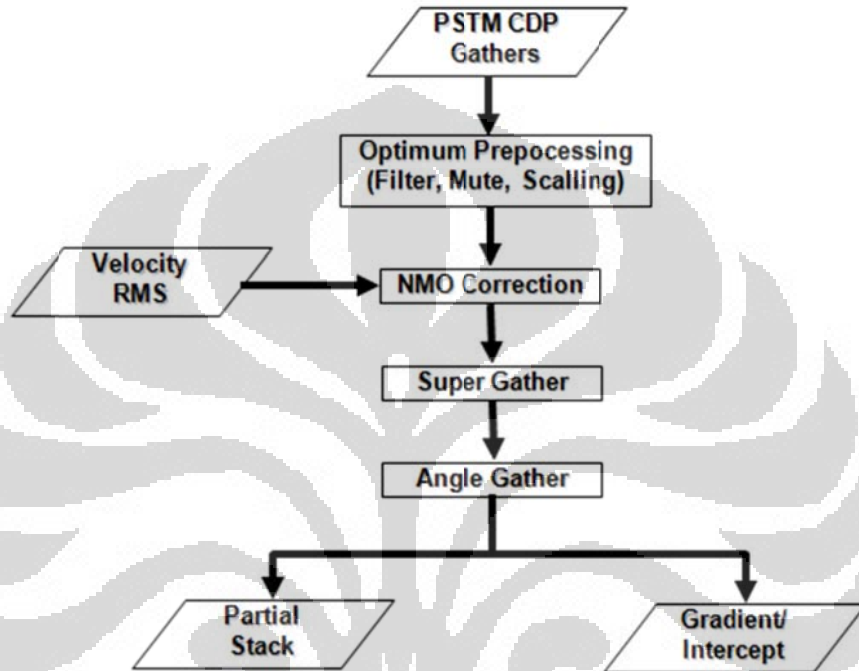


Figure 2.1 Flow chart for AVO analysis

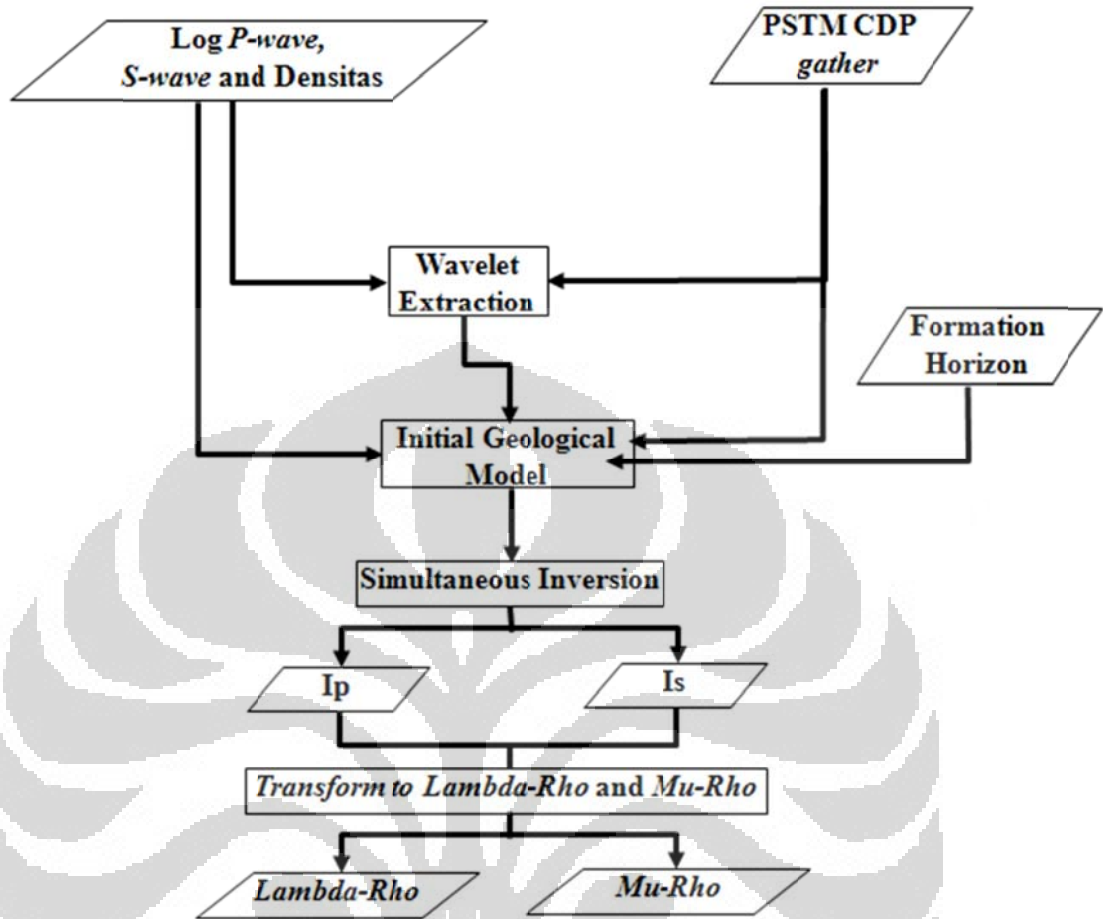


Figure 2.2 Simultaneous inversion flow chart

CHAPTER 3

BASIC THEORY

3.1. Amplitude Variation with Offset (AVO) Analysis

3.1.1. Basic Principal of AVO Method

Elementary principle of AVO method (Amplitude of Variation with Offset) is to analyze the change of amplitude from reflected wave to incidence angle (Allen and Peddy, 1993).

Offset is having direct correlations to incidence angle (angle of incident) with reflector layer. If offset is bigger, then the incidence angle too will have a large value. It's shown by figure 3.1

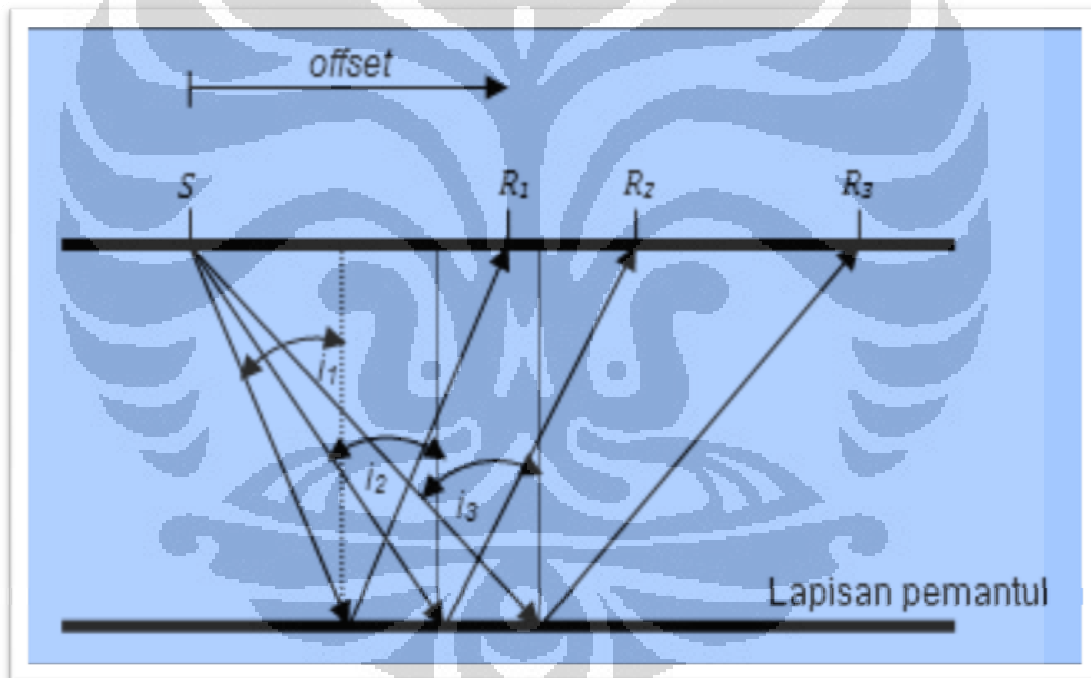


Figure 3.1 relationship between offset and incidence angle

Hydrocarbon Attendance effect in medium result the AVO anomaly that is assorted change of P wave amplitude to offset

3.1.2. Reflected Coefficient of zero Incidence Angle

Comparison between reflected amplitude with the amplitude incidence wave called as reflected coefficient, while reflected coefficient of zero incidence angles is the wave that perpendicular to the reflector area. Figure 3.2 showing the

illustration of reflected coefficient at zero incidence angles.

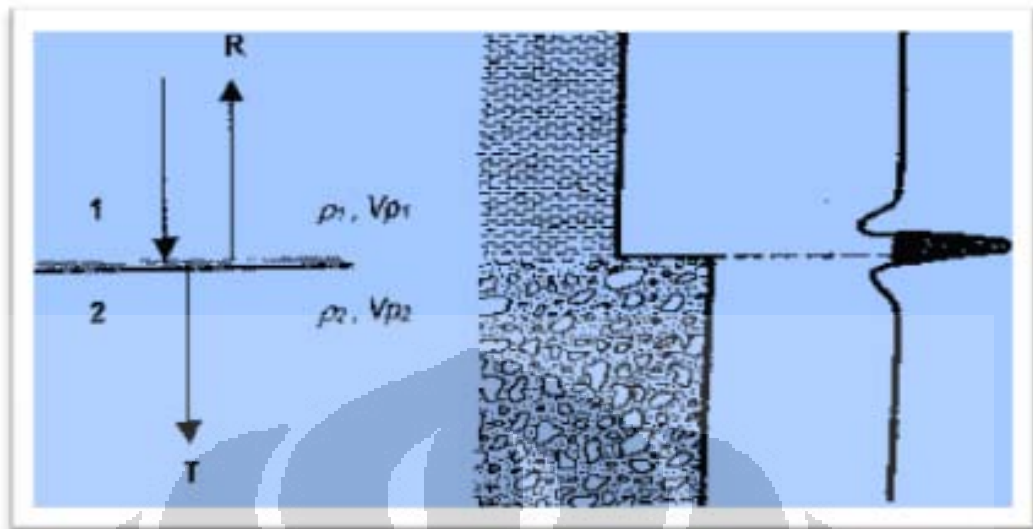


Figure 3.2, Reflected Coefficient of zero incidence angle.

Reflected coefficient of P wave of P at zero incidence angle R_0 is

$$R_0 = \frac{A_1}{A_0} = \frac{\rho_2 V_{P2} - \rho_1 V_{P1}}{\rho_1 V_{P1} + \rho_2 V_{P2}} \quad (3.1)$$

With, R_0 = reflected coefficient of zero incidence angle

A_1 = reflected amplitude wave at 1st medium

A_0 = incidence amplitude wave

ρ_1 = 1st medium density

ρ_2 = 2nd medium density

V_{P1} = 1st medium velocity of P wave

V_{P2} = 2nd medium velocity of P wave

$\rho V_P = Z =$ acoustic impedance

Reflected coefficient based on polarity according to Society of Exploration Geophysics (SEG) divided into two term, that is normal polarity (polarity) and the inversed polarity (reverse polarity). Figure 3.3.(a) showing normal polarity and the inversed polarity for the minimum phase wavelet and (b) zero phase wavelet.

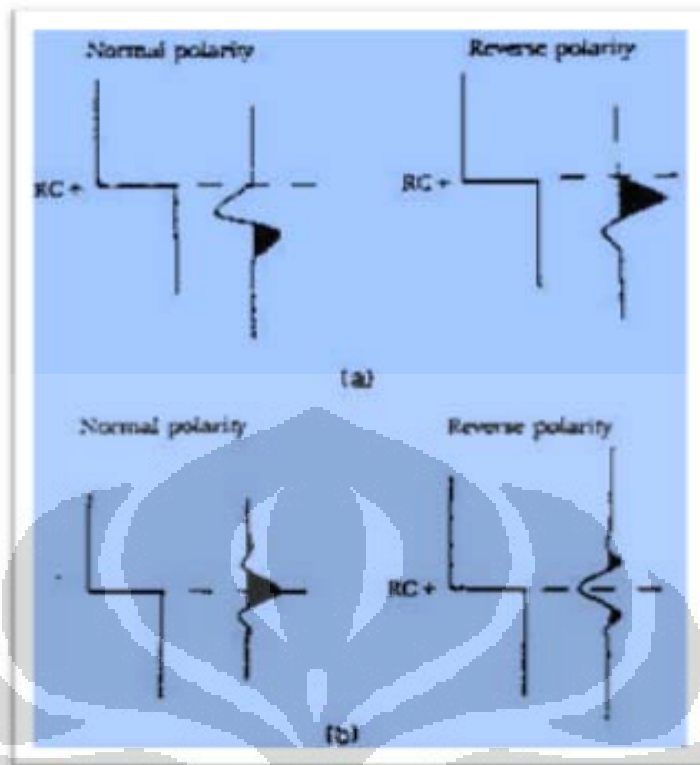


Figure 3.3, (a) normal polarity and reverse polarity for the minimum phase wavelet and (b) zero phase wavelet

3.1.3. Poisson's Ratio

Poisson ratio is defined as a comparison between radial strain and axial strain. This parameter connects the fraction of diameter change with the fraction of length change in a cylindrical substance (Figure 3.4). The Poisson ratio can be writing as below,

$$\sigma = \frac{\Delta R/R}{\Delta L/L} \quad (3.2)$$

with ,

σ = Poisson ratio

ΔR = change in the half of cylindrical diameter (cm)

R = half of cylindrical diameter (cm)

ΔL = change in the length of cylinder (cm)

L = length of cylinder (cm)

Poisson ratio has a relationship with the P wave and S wave velocity, which is,

$$\sigma = \frac{1}{2} \left(\frac{V_P^2 - 2V_S^2}{V_P^2 - V_S^2} \right) \quad (3.3)$$

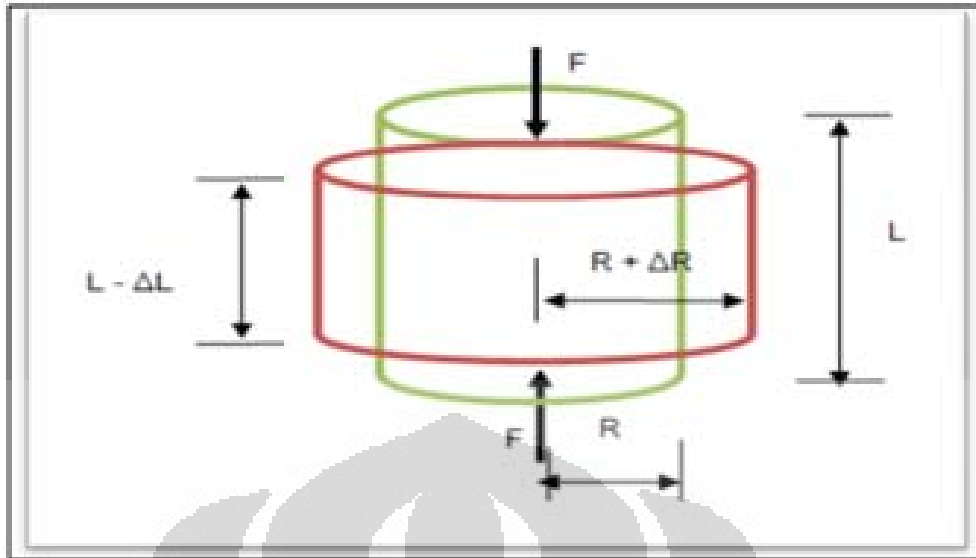


Figure 3.4, A cylinder with the pressure at its top and bottom of cylinder.

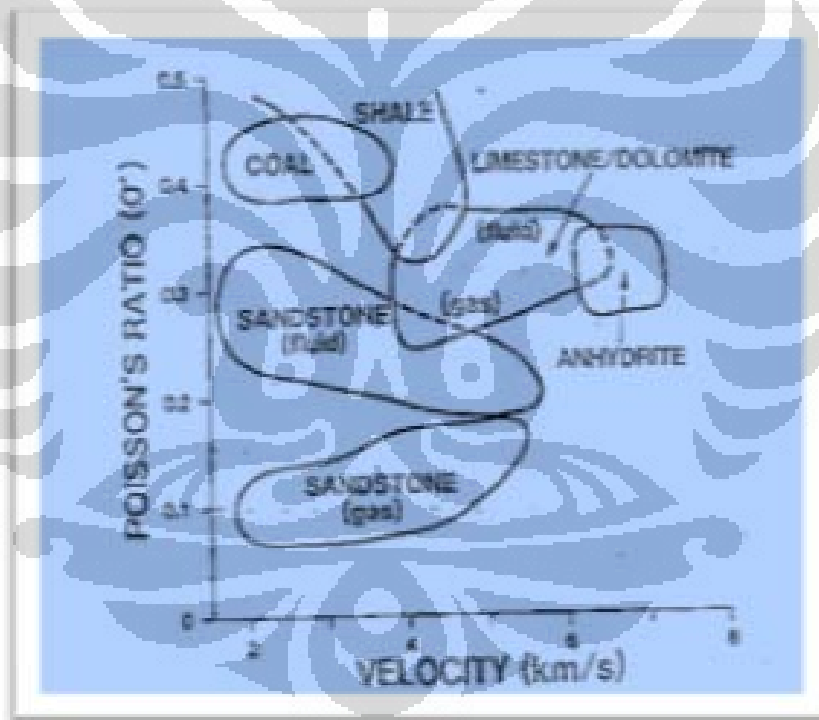


Figure 3.5, Poisson ratio value based on the medium (Wren,1984) .

Poisson ratio has a value between 0 – 0.5, it depends on the media that passed by the wave. Gas sand Poisson ratio value is in range of 0.07 – 0.19. This was caused by different between P wave and S wave velocity. Figure 3.5 shows the range of Poisson ratio value in the medium against velocity.

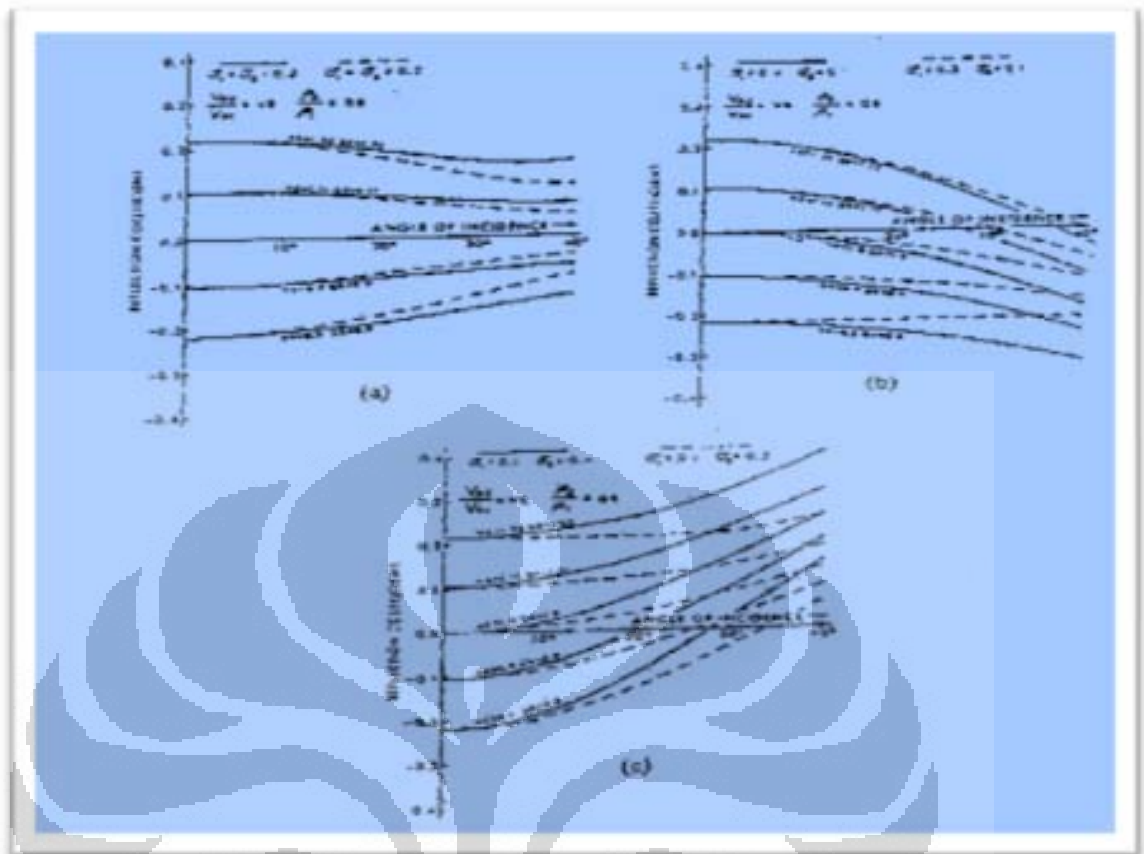


Figure 3.6. Plot of P wave reflected coefficient versus incidence on the interface for Poisson ratio at 0.2 and 0.3 (a), depleted Poisson ratio (b) and Increased Poisson ratio (c) (Ostrander, 1984).

Ostrander (1984) proposed that ratio Poisson has an influence to reflected coefficient change as incidence angle function. Figure 3.6(a) explaining the alteration of P wave reflected coefficient as a function of incidence angle at interface with Poisson ratio constant in range 0.2 and 0.3.

Figure 3.6(b) show the alteration of P wave reflected coefficient with Poisson ratio medium value. Straight line at curve show Poisson ratio value 0.4 – 0.1 and the dash line have Poisson ratio value 0.3 – 0.1. From the picture above that the Poisson ratio and reflected coefficient will drop as the incidence angle increase, its mean that reflected coefficient has positive value with reverse polarity and reflected coefficient value will increase as the incidence angle higher.

Figure 3.6(c) is a contrary from figure 3.6(b), that the Poisson ratio value decreases. From the curve in figure above, it can conclude that when the incidence

value higher, P wave reflected coefficient increase. It's a meaning that the reflected coefficient having a negative value with inversed polarity and the value of reflected coefficient is increasing with the incidence angle higher.

3.1.4. Simplification of Zoeppritz Equation

Simplification of Zoeppritz Equation used in this research is a simplification equation by Shuey (1985). This approach is assistive in the interpretation of AVO and gives a simple relationship between rocks parameters, in example the alteration of Poisson ratio, incidence angle and also the variation of reflected coefficient. Simplification of Zoeppritz Equation by Shuey (1985) is shown in equation below:

$$R(\theta) = R_0 + \left(A_0 R_0 + \frac{\Delta\sigma}{(1-\sigma)^2} \right) \sin^2 \theta + \frac{1}{2} \frac{\Delta V_p}{V_p} (\tan^2 \theta - \sin^2 \theta) \quad (3.4)$$

With $R(\theta)$ = P wave reflected coefficient as an incidence function (θ).

$$R_0 = \frac{1}{2} \left(\frac{\Delta V_p}{V_p} + \frac{\Delta\rho}{\rho} \right) = \text{reflected coefficient at zero incidence} \quad (3.5)$$

$$A_0 = B_0 - 2(1 - B_0) \frac{1-2\sigma}{\sigma} = \text{amplitude of source wave}$$

Where as
$$B_0 = \frac{\Delta V_p / V_p}{(\Delta V_p / V_p) + (\Delta\rho / \rho)}$$

$\Delta\sigma = \sigma_2 - \sigma_1$ = the difference between Poisson ratio at medium 2 with medium 1

$\sigma = (\sigma_1 + \sigma_2)/2$ = the average value of Poisson ratio at medium 2 with medium 1

$\Delta V_p = V_{p2} - V_{p1}$ = the difference of Velocity of P wave at medium 2 with medium 1

$V_p = (V_{p2} + V_{p1})/2$ = the average value of P wave velocity at medium 2 with medium 1

The Shuey Equation consisted of three parts, first part is (R_0) which expressing the reflected coefficient at zero incidence angle, second part

show at middle incidence angle ($0^\circ < \theta < 30^\circ$), and the third part is near critical angle. If θ minimum then $\sin^2\theta \approx \tan^2\theta$ so that the third part is equal to zero, equation (3.5) becoming:

$$R(\theta) = A + B \sin^2 \theta \quad (3.6)$$

Equation (3.6) above is often used in the analysis AVO, with A represent the reflected coefficient of zero incidence angle (R_0), while B represent the alteration of reflected amplitude to the increasing $\sin^2\theta$, which is called gradient (slope) AVO, whereas,

$$G = A_0 R_0 + \frac{\Delta\sigma}{(1+\sigma)^2} \quad (3.7)$$

3.1.5. Gas Detection on Medium

So far, AVO method is a method that most pre-eminent in detecting the existence of gas sand.

The characteristic of low value in gas sand for VP/VS can differentiate layering that having low impedance such as coal and porous brine sand.

The last analysis method of AVO (Rutherford And William, 1989) indicating that layering gas sand doesn't always cause reflected amplitude of P wave increase to offset, however various alteration variation of reflected amplitude of P wave to offset.

Rutherford and William (1989) was categorized the gas sand into 3 by the characteristic respond in AVO, which are :

1. Gas Sand Class 1, which is sand gas that has higher acoustic impedance than shale above, with zero positive for reflected coefficient at incidence.
2. Gas Sand Class kelas 2, which is sand gas that has acoustic impedance value relatively the same with the shale above and reflected coefficient approaching zero.
3. Gas Sand Class 3, which is sand gas that has lower acoustic impedance than shale above with zero negative for reflected coefficient at incidence.

Ross and Kinman (1995) modified the classification by Rutherford dan William (1989) by divided Class II into Class II and Iip, then Castagna (1997) added the Class IV, so therefore the characteristic of reservoir become:

1. Class I : High contrast acoustic impedance
2. Class II : Near zero contrast acoustic impedance
3. Class Iip : Near zero contrast acoustic impedance with polarity change
4. Class III : Low contrast acoustic impedance
5. Class IV : Low contrast acoustic impedance and higher amplitude value as offset increase.

The characteristic of AVO for each class is showed in figure 3.7.

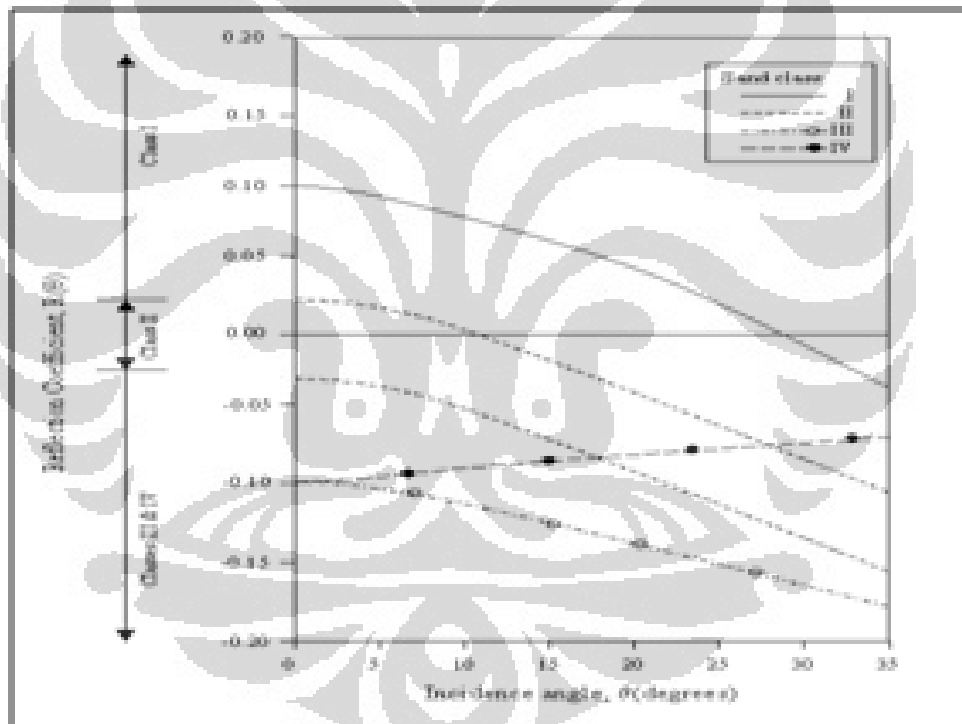


Figure 3.7 Sand category based on AVO characteristic

3.1.6. AVO Attributes

Attribute AVO is a method to analyze the alteration of signal amplitude that reflected with the increasing in ofsett or the incidence angle (Ahmed, 1991) and refer to the equation given by Shuey (1985) that consisted of:

1. *Intercept (A)* :Intercept attribute is the value of reflected amplitude at zero offset or reflected coefficients at normal incidence angle. This is shown in equation (3.6)
2. *Gradient (B)*: Gradient attribute is the alteration value of relative amplitude with the square of sinus of incidence or offset, shown by equation (3.7). If perceived, this attribute does not give information about decreasing or increasing amplitude to offset. To know its influence, this attribute is used at the same time with first attribute (intercept).
3. *Intercept * Gradient (A*B)*: Intercept*Gradient Attribute is the multiplication between intercept with gradient and used as an indicator the present of gas. An increasing of absolute amplitude to offset will be obtained if the result of this multiplication from this factor is positive, a decreasing of absolute amplitude to offset will be obtained if the result of this multiplication from this factor is negative, while for the constant absolute amplitude to offset] if its multiplication equal to zero.
4. *Gradient * A-sign*: Gradient*A-Sign Attribute is the multiplication between gradient with the sign owned by intercept, regardless the value of A. Result of negative multiplication indicate that both parameter have adversative sign, while positive value show this parameters have the same sign. Level value of this multiplication result is only determined by the value of gradient..
5. Scaled Poisson ratio: Scaled Poisson ratio attribute to incidence angle illustrate the increase and decrease of Poisson ratio at each lihtology.
6. *Crossplot*: Crossplot attribute is the simple way to present the modeling of AVO data. Data Information that cannot be seen by the appearance on offset and will be able to be presented in cross plot. Amplitude variation to offset for reflected boundary is presented as single dot at intercept and gradient crossplot. At this attribute, it can be determine the area that contains gas and oil, from the cluster of data intercept and gradient crossplot.
7. *crossplot Section*: Crossplot section attribute is representing the result of crossplot attribute in the form of section. Anomali zoning of amplitude

from crossplot attribute can be gas and oil, will be depicted precisely at CDP gather section. This attribute will present the boundary from each layering that contains oil and gas.

3.2. Lambda-Mu-Rho (LMR) Attribute

3.2.1. Definition of LMR

Lambda-Mu-Rho (LMR) Attribute concept was defined by Goodway et al (1997). The concept is using the elastic parameter of rock as optimum indicator for lithology change and hydrocarbon fluid. Constant Lamé parameter λ , μ dan ρ is incompressibility, rigidity and density of rocks. Gray and Andersen (2000) explain that the modulus shift (μ or rigidity) is defined as the persistency of rocks to a strain that resulted in transformation, but did not change the total volume of rocks. Rigidity is very useful to differentiate the quality of lithology because in general, it's not influenced by fluid of reservoir. Lambda Modulus (λ) will be interconnected with incompressibility at rocks medium. Lambda parameter (λ) give information about fluid content at rocks pore. Incompressibility is also conceived as bulk modulus that is persistency of rocks to volume change which is caused of the pressure change. Incompressibility has reverse meaning as compressibility. Figure 3.8 explaining some condition of rocks matrix in normal condition, compressed and pressure shift. Figure 3.8(a) showing of rock matrix at normal condition without pressure, compressed by pressure (figure 3.8(b)) hence space of pore among matrix will decrease. If the pore fill by fluid (for example: oil or brine) hence the fluid will act as persistent so that the rock will become more incompressible. But if fluid inside the matrix is gas hence value of incompressibility of rock will low. This matter is caused by gas persistent is not like as oil or brine. If matrix of rock incurred by the pressure shift like shown at figure 3.8(c), hence matrix of rock will be shifted or equally will be transformed. The more rigid of rocks, hence will difficult to be transformed. At this case of pressure shift, rocks matrix did not influenced by fluid effect Royle, (1999).

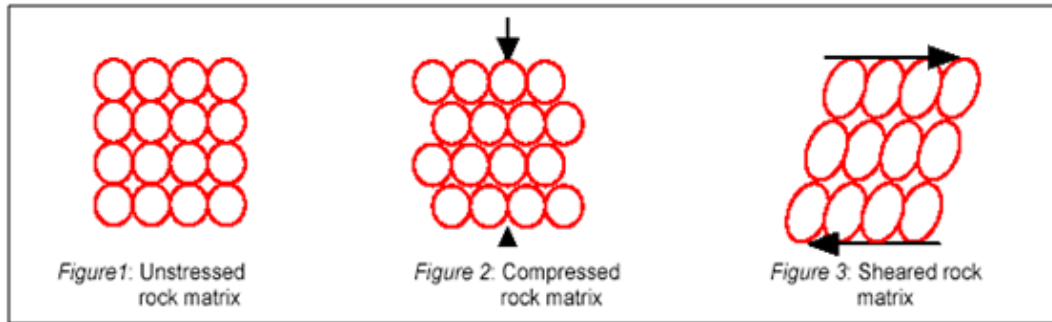


Figure 3.8, illustration of rocks matrix
 (a) normal condition, (b) compressed and (c) pressure shifted (Royle, 1999)

3.2.2. Goodway Approximations

Goodway Et al (1997) introducing use of modulus shift constant and Lamé constant ($\lambda\rho$ and $\mu\rho$) as indicator of lithology and fluid. From the relation of P impedance (IP) and S impedance (IS) with density and also velocity of P wave and S wave,

$$I_P = V_P \rho \quad (3.8)$$

$$I_S = V_S \rho \quad (3.9)$$

Relationship between velocity of P wave and S wave with Lamé constant as

$$\text{below, } V_P = \sqrt{\frac{\lambda + 2\mu}{\rho}} \quad (3.10)$$

$$V_S = \sqrt{\frac{\mu}{\rho}} \quad (3.11)$$

Afterward substitute the equation above in to equation of P impedance and S impedance, it will become,

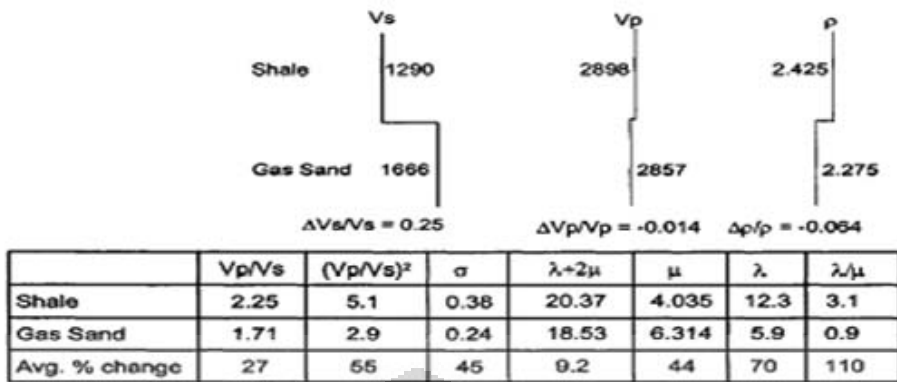
$$\lambda = I_P^2 - 2I_S^2 \quad (3.12)$$

$$\mu\rho = I_S^2 \quad (3.13)$$

From equation (3.12) and (3.13) can be seen that parameter $\lambda\rho$ dan $\mu\rho$ is a function of square from P impedance (IP) and S impedance (IS), its mean that small anomaly from P impedance (IP) and S impedance (IS) will become big at Lamé parameter (λ and μ). Lithology and fluid Detection using this physics parameter show more value, as seen at Tables 3.1. Sensitivity Change that expressed in Lamé parameter gives highest result.

Tabel 3.1 sensitivity analysis using petrophysics (Goodway et al, 1997)

Improved AVO using Lamé parameters: " $\lambda\rho$ ", " $\mu\rho$ " & " λ/μ fluid stack".



Goodway Et al (1997) describes comparison crossplot between log Lambda-Mu-Rho and impedance. Figure 3.9 show crossplot Lambda-Mu-Rho parameter give more significant data group division compared to impedance crossplot. At impedance crossplot (figure 3.9), P impedance value among solid sand and gas sand still overlap, also for shale and sand. But at LMR parameter crossplot, the cut off between gas sand with lithologi dissimilarity seen more coherent.

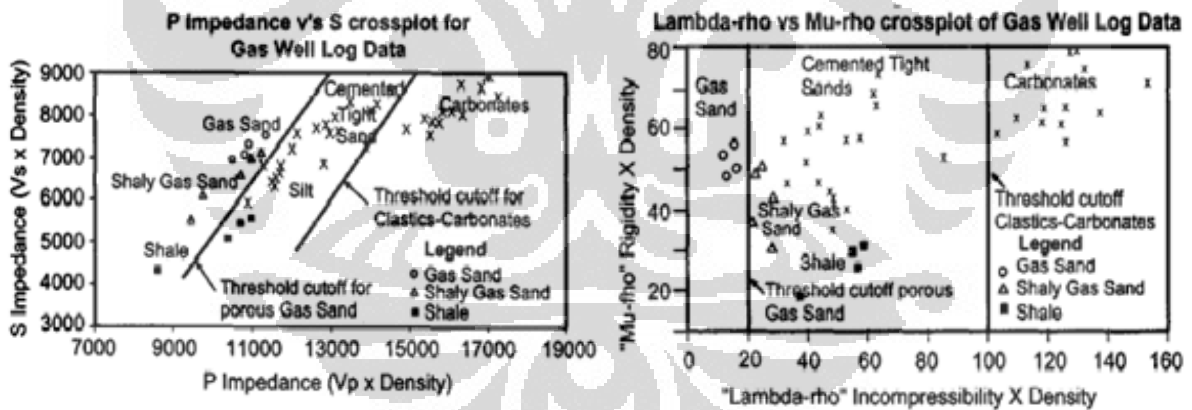


Figure 3.9 the comparison between crossplot of P impedance vs S impedance log and crossplot Lambda-Rho vs Mu-Rho (Goodway et al, 1997)

Figure 3.9 show cut-off of Lambda-Rho between shale and gas sand is 20 GPA. This also means that with Lambda-Mu-Rho parameter will give clearer definition of anomaly zoning. While at impedance crossplot, the impedance cut off makes a diagonally pattern, so there will be an overlapped for a few lithology.

CHAPTER IV

PROCESSED DATA AND ANALYSIS

4.1. LOG PROPERTY CROSS-PLOTS

Cross-plotting two logs with a third log as color attribute helps in determining the sensitivity of petrophysical properties. For NSH-1 well, three type of cross plot with different color codes is done.

4.1.1. V_p versus V_s

Cross-plotting V_p versus V_s , we can see most of the data lies on a 45-degree trend, representing the wet case.

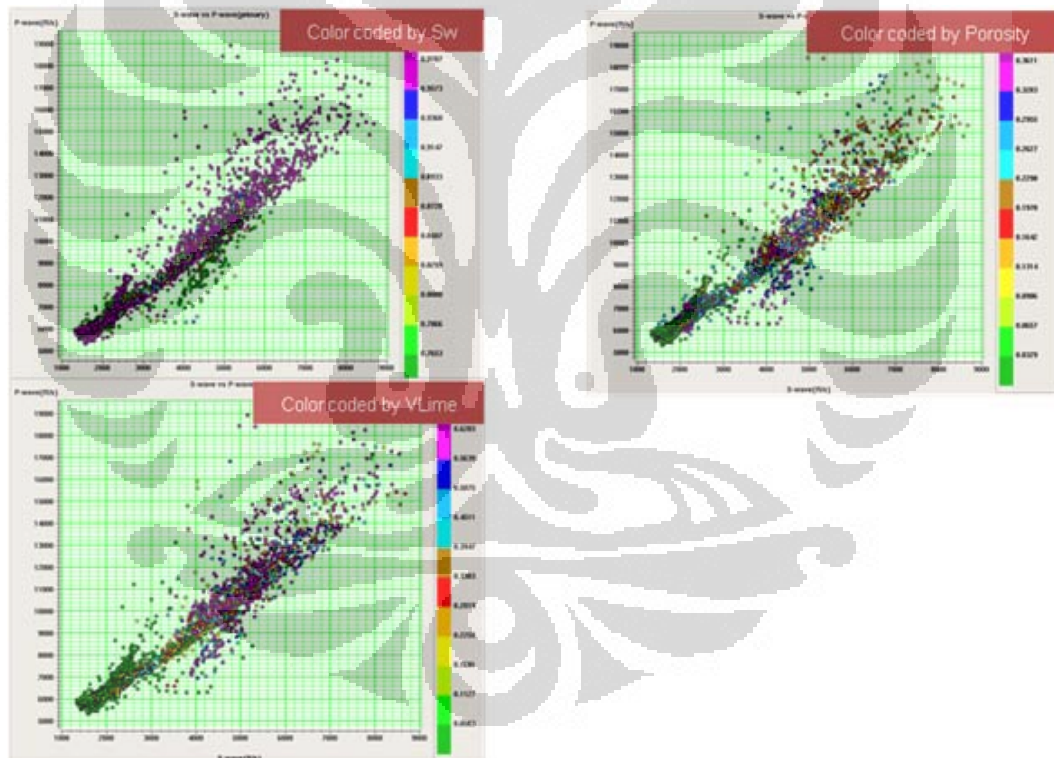


Figure 4.1. NSH-1 Well Cross plot of V_p versus V_s , color coded by different petrophysical logs

A few anomalous points lie below the line (i.e have a lower V_p/V_s ratio) and these also correlate with the gas zone in the Kujung1, above the GWC.

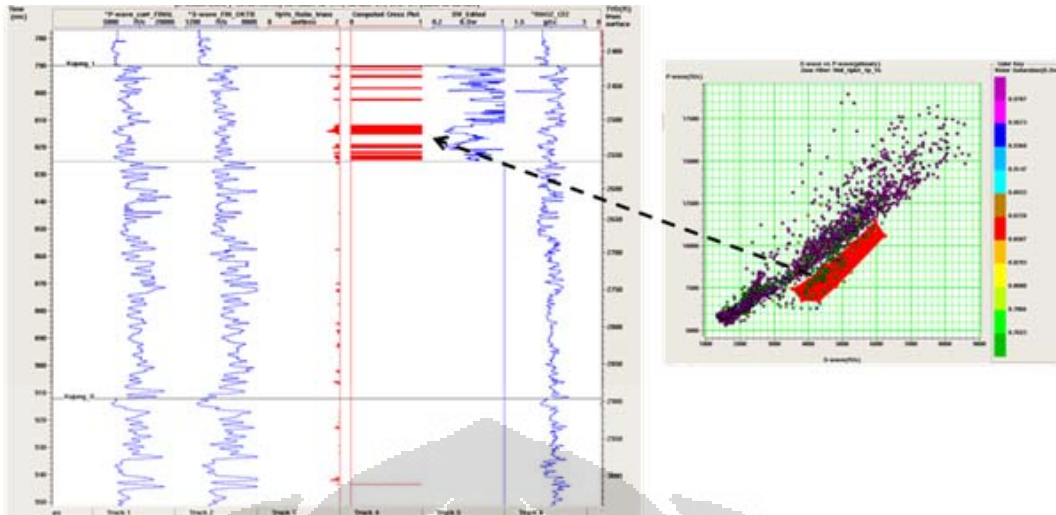


Figure 42. NSH-1 Well Cross plot of V_p versus V_s showing zone that highlighted the HC anomaly

4.1.2. Z_p versus V_p/V_s Ratio

Cross-plotting Z_p versus V_p/V_s , we can see most of the data lies in a rotated hyperbola curve, with a few outliers at low Z_p and low V_p/V_s .

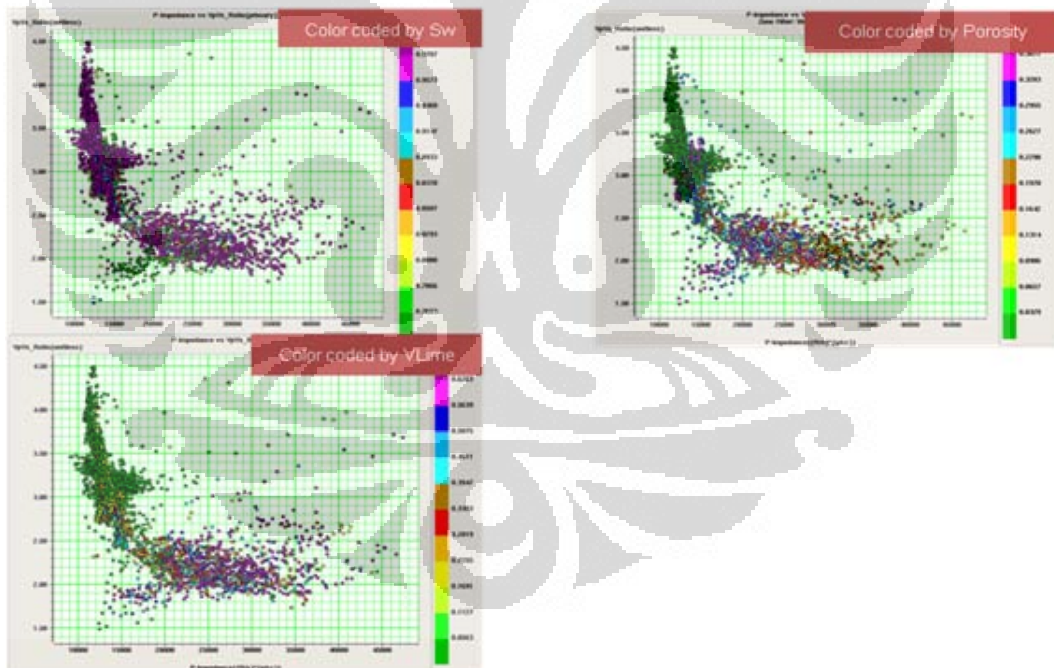


Figure 4.3. Well Cross plot of Z_p versus V_p/V_s , color coded by different logs

Similar to the previous cross-plot, these anomalous points correlate with the gas zone in the Kujung1, above the GWC.

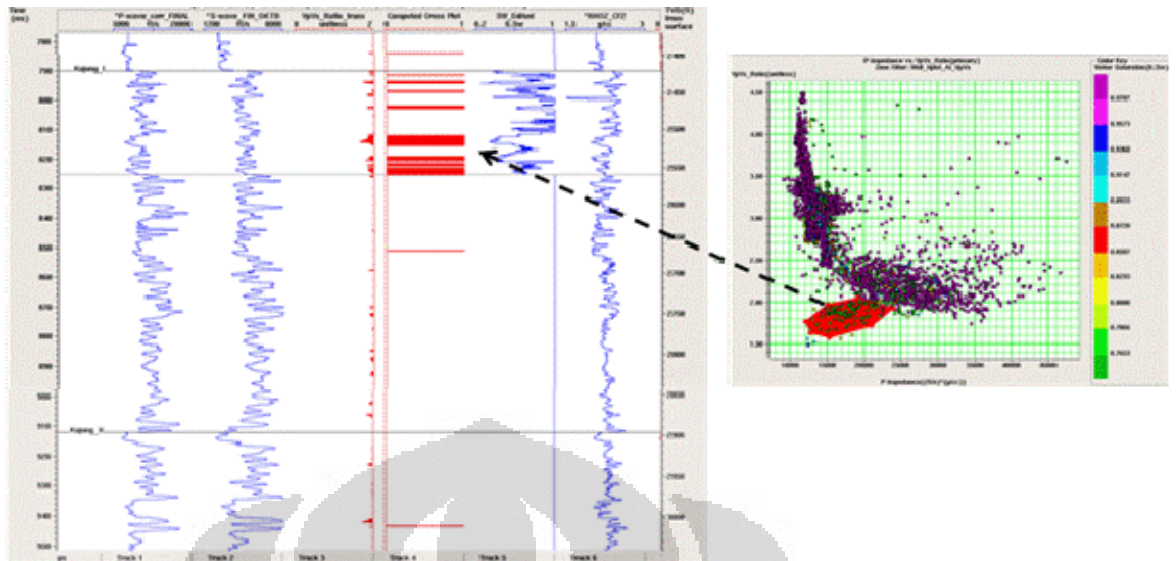


Figure 4.4. NSH-1 Well Cross plot of Z_p versus V_p/V_s showing zone that highlighted the HC anomaly

4.1.3. V_p versus Density

The V_p and Density cross-plot look normal and indicate that the Density of reasonable quality.

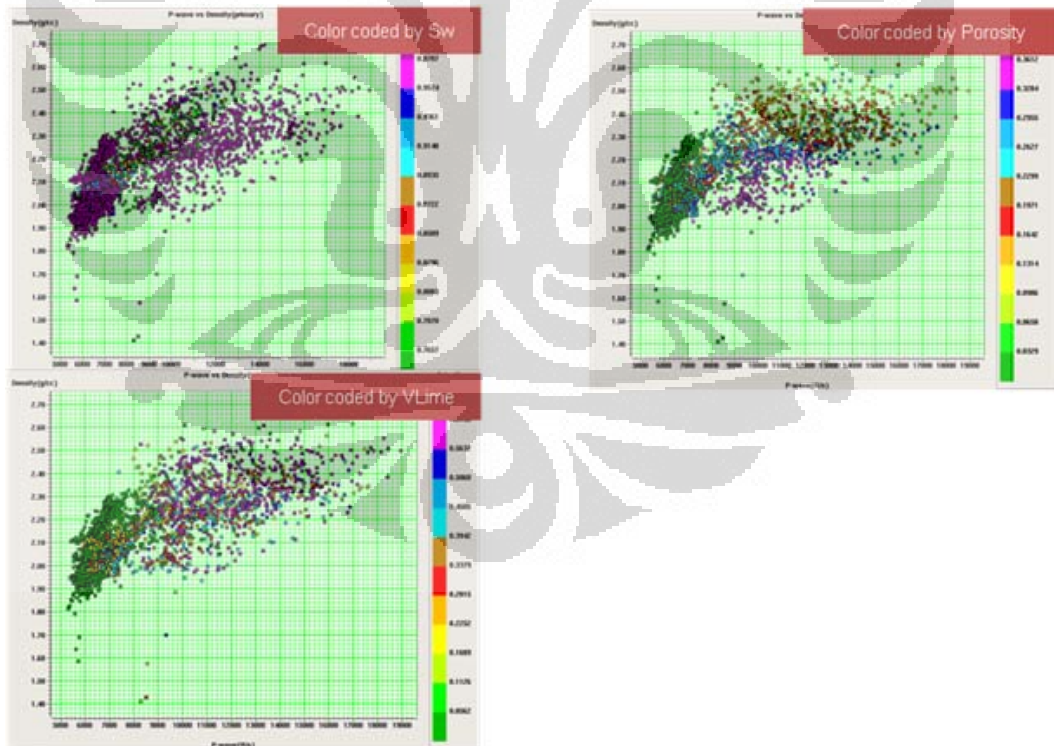


Figure 4.5. NSH-1 Well Cross plot of V_p versus Density, color coded by different logs

4.1.4. LMR Logs

The P-Impedance and S-Impedance well logs were transformed to Lambda-Rho and Mu-Rho logs. This transform highlights errors in the velocity logs and, in this well, it appears that the two well logs are good.

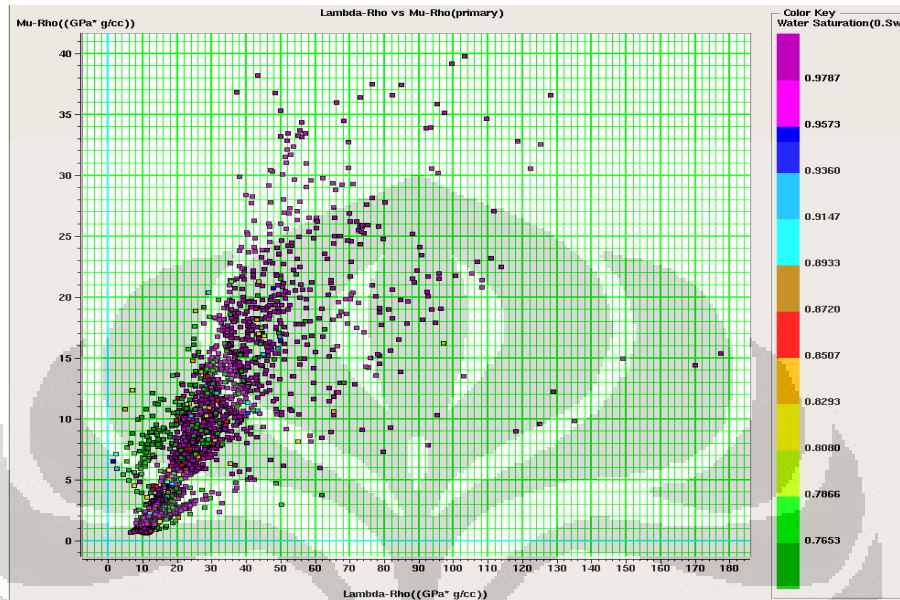


Figure 4.6. NSH-1 Well Cross plot of LR versus MR, color coded by Water Saturation

The anomalous zone highlighted by the low Sw values in the cross-plot project onto the gas zone above the GWC in Kujung 1.

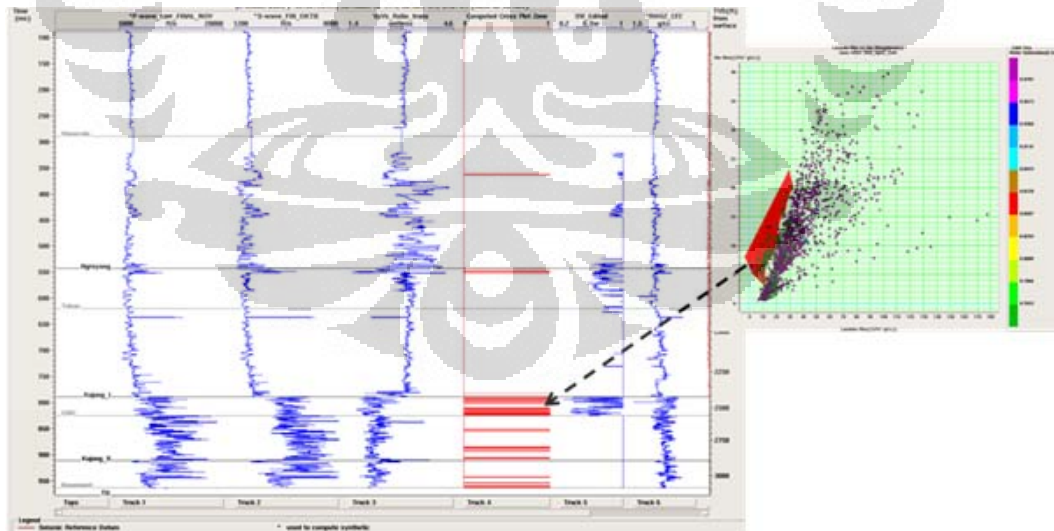


Figure 4.7. NSH-1 Well Cross plot of LR versus MR, showing zone that highlighted the HC anomaly

4.2. WELL SEISMIC TIE

A critical requirement in all future processing steps is that the well logs tie accurately to the seismic volumes. Well logs are measured in terms of depth units (i.e., feet) as the well log tool is moving up along the well bore. The seismic data, however, is measured in two-way travel time beginning from the detonation of the seismic source, continuing as the seismic ray travels through the sub-surface and measured when it is received at the hydrophone or geophone receiver. The transformation process to convert the depth measurements of the well logs to the seismic travel times requires a table that maps each depth to a two-way travel time. This mapping table is called the depth-time table.

An additional essential requirement is that, in order to create the synthetic seismic trace, the wavelet is known. In this case, the wavelet is not known and so an estimate of the wavelet must be attempted. In order for the wavelet to be estimated accurately, the well must correlate exactly with the seismic. This results in an iterative process of both well-seismic correlation and wavelet estimation. That is, an initial wavelet is estimated, the well is correlated, another wavelet is estimated using the well log reflectivity to estimate the phase, and the correlation process is repeated with the new synthetic trace.

4.2.1. Applying Check-shot correction

After all the elastic logs (DT, DTS and Density) have been corrected, we can now correlate the logs (measured in depth) with the seismic (measured in time). Check-shots were available and a correction to honor the check-shot data was first applied to the calculated TZ curves. Note that there are no check-shot measurements beyond 2750 ft to the bottom of the hole.

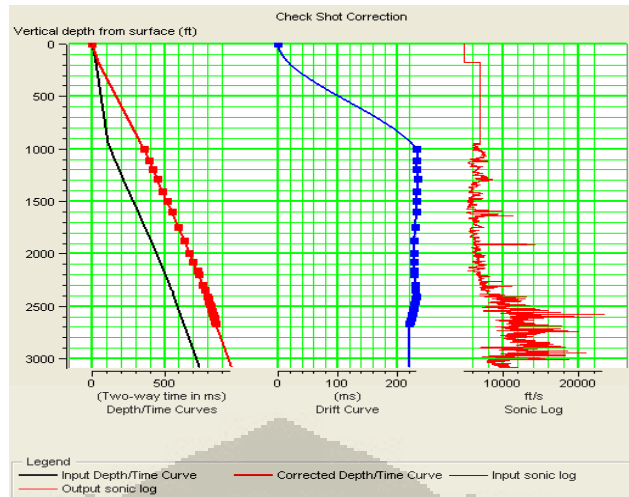


Figure 4.8. Displaying the check shot data

4.2.2. Statistical Wavelet Extraction

A statistical wavelet was extracted from around the well, including the zone of interest. This wavelet is used in the initial well log correlation. Below is the final wavelet used.

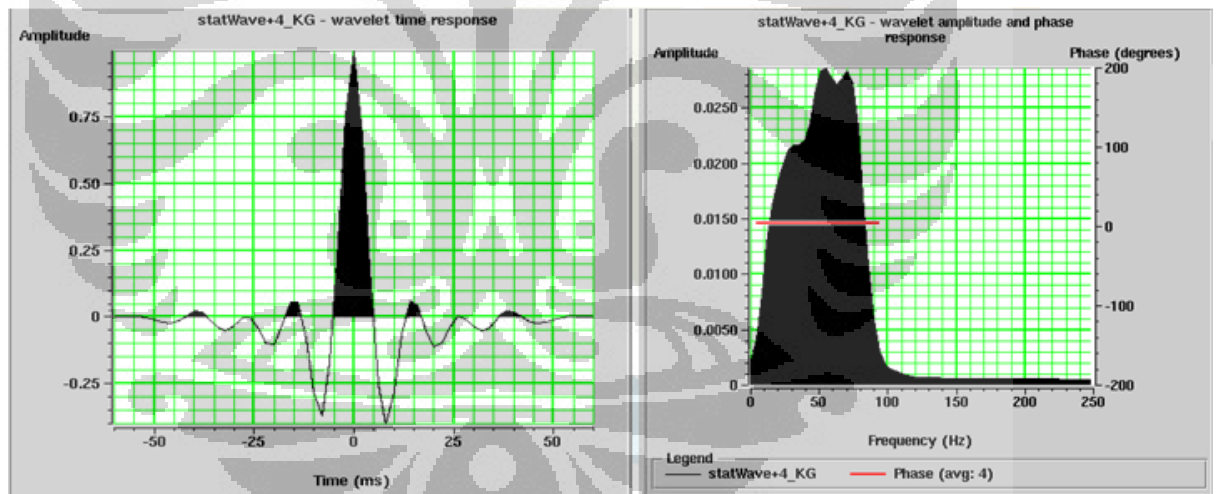


Figure 4.9. Statistical Wavelet used in the Well Correlation process

4.2.3. Seismic Well Correlation

The well to seismic correlation detailed steps are as follows:

- Initial Correlation after Check-shot correction was -11.4 %. Notice that check-shot does not reach TD (Figure 10)
- Correlated on two strongest events: NGRAYONG and KUJUNG1.
Applied Stretch to time-depth curve (Figure 11)

- After fixing the NGRAYONG and KUJUNG1 picks, correlated events below the check-shot log. Applied stretch (Figure 12)
- After +4 degree wavelet phase rotation, the final correlation is now 49 %, from NGRAYONG -100 ms to BASEMENT (Figure 13)

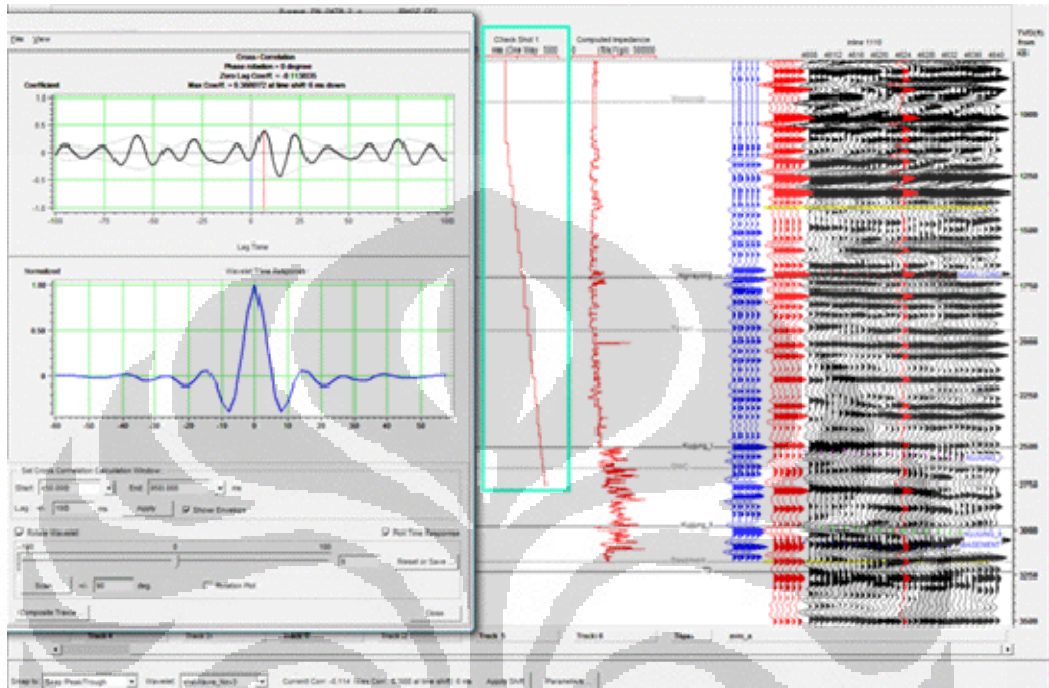


Figure 4.10. Initial correlation after check-shot correction was -11.4%. Notice that check-shot does not reach TD

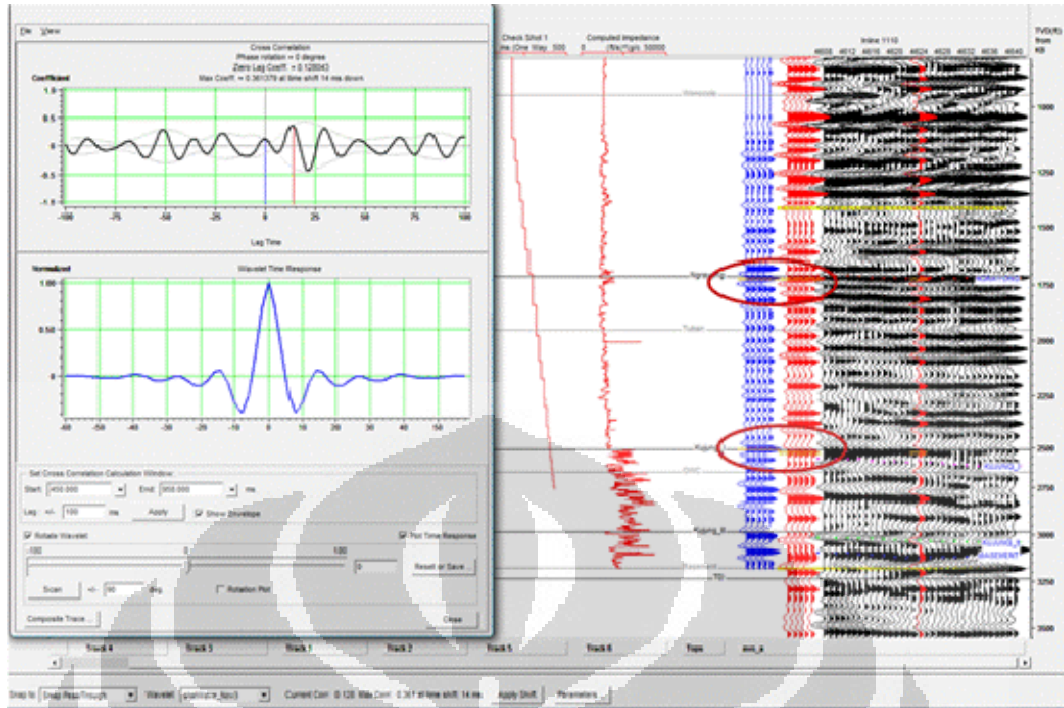


Figure 4.11. Correlated on two strongest events: NGRAYONG and KIJUNG1. Applied stretch to time-depth curve

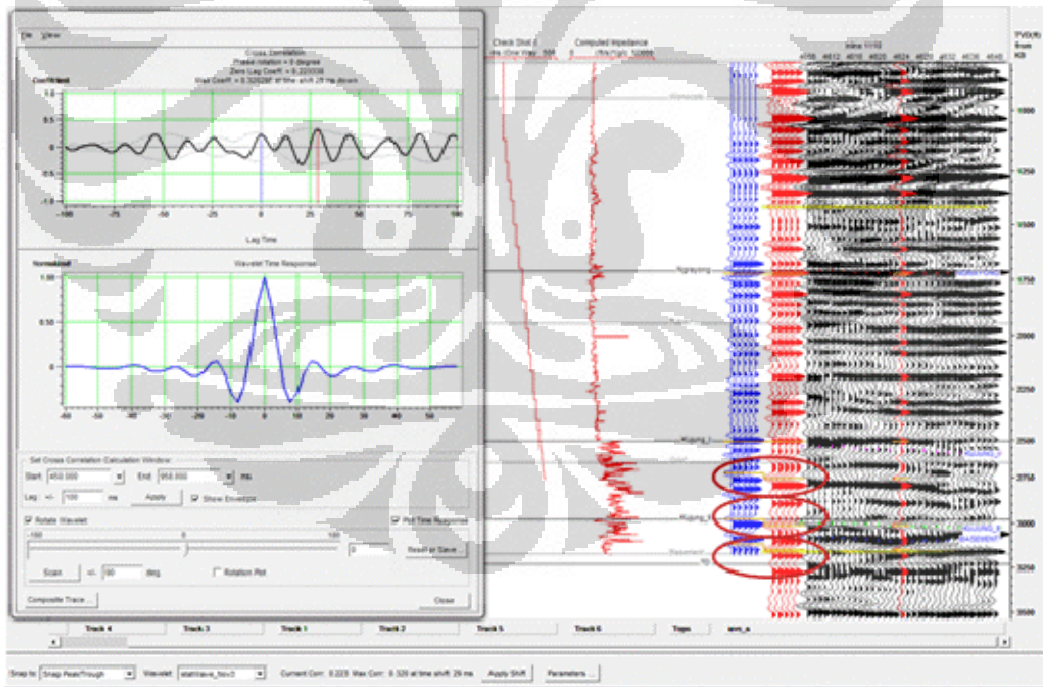


Figure 4.12. After fixing the NGRAYONG and KIJUNG 1 picks, correlated events below the check-shot log. Applied stretch

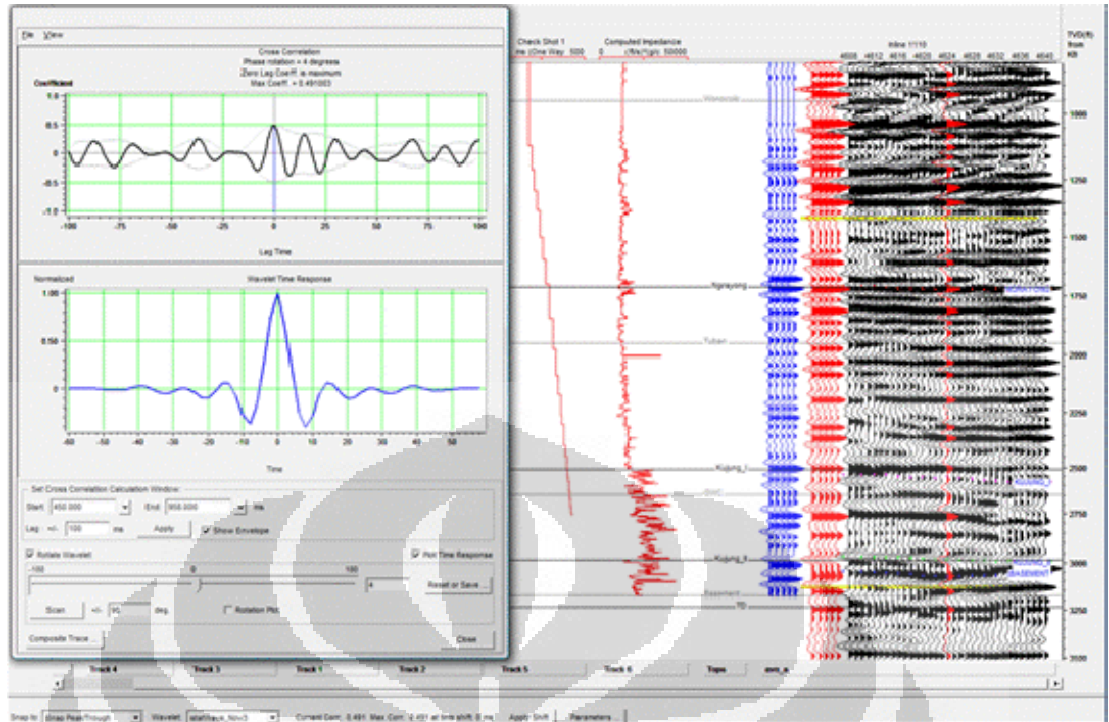


Figure 4.13. After slight +4 degree wavelet phase rotation, the final correlation is now 49% from NGRAYONG -100 ms o BASEMENT

4.3. SEISMIC DATA LOADING AND CONDITIONING

4.3.1. Loading NMO Corrected Gathers

The data received is an NMO Corrected Gathers as shown below.

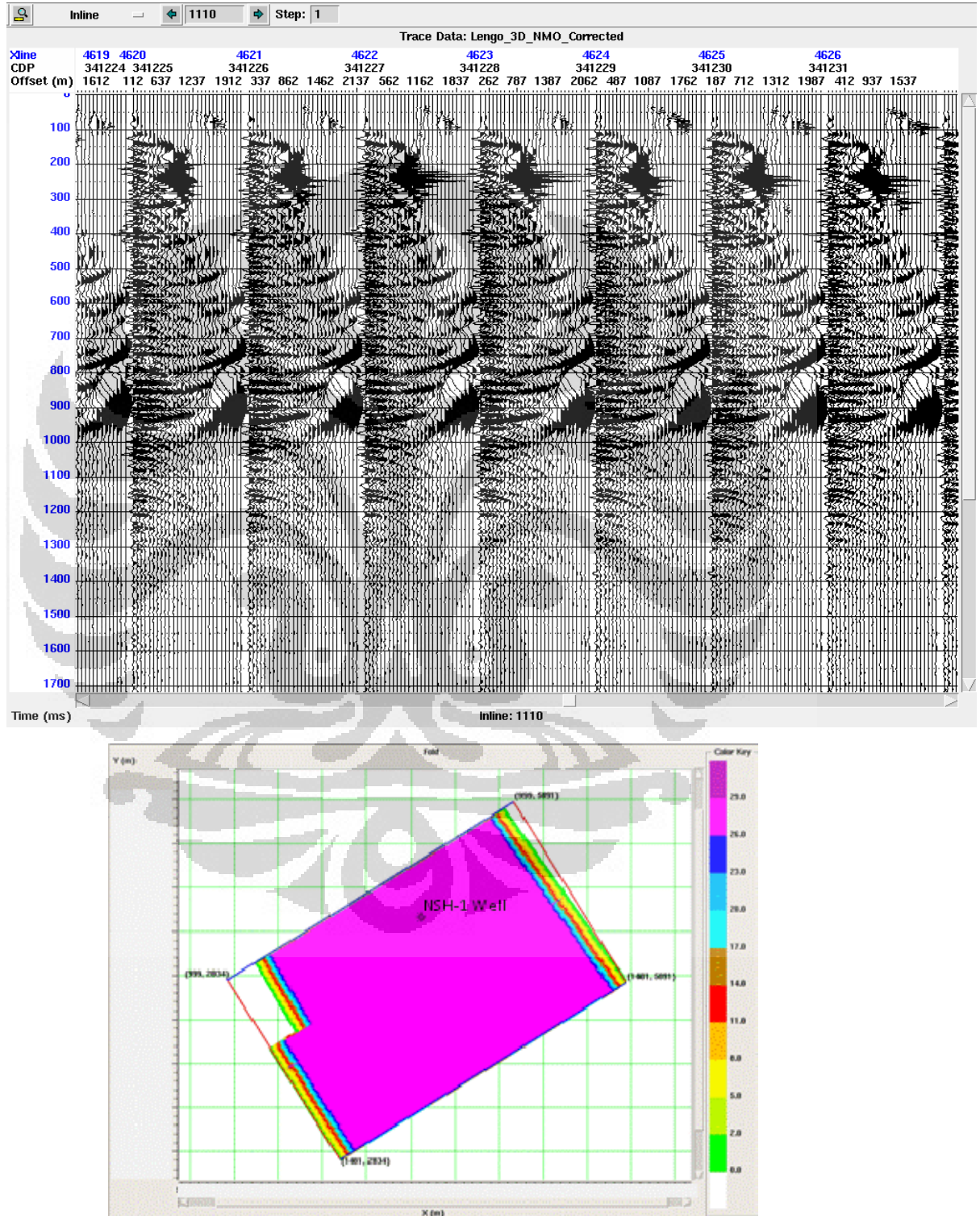


Figure 4.14. NMO Corrected Gathers and the 3D Basemap showing fold

4.3.2. Determining Seismic Polarity

After examining the data for the sea bottom reflection, we conclude that the wavelet polarity used is: Increase in AI = Peak.

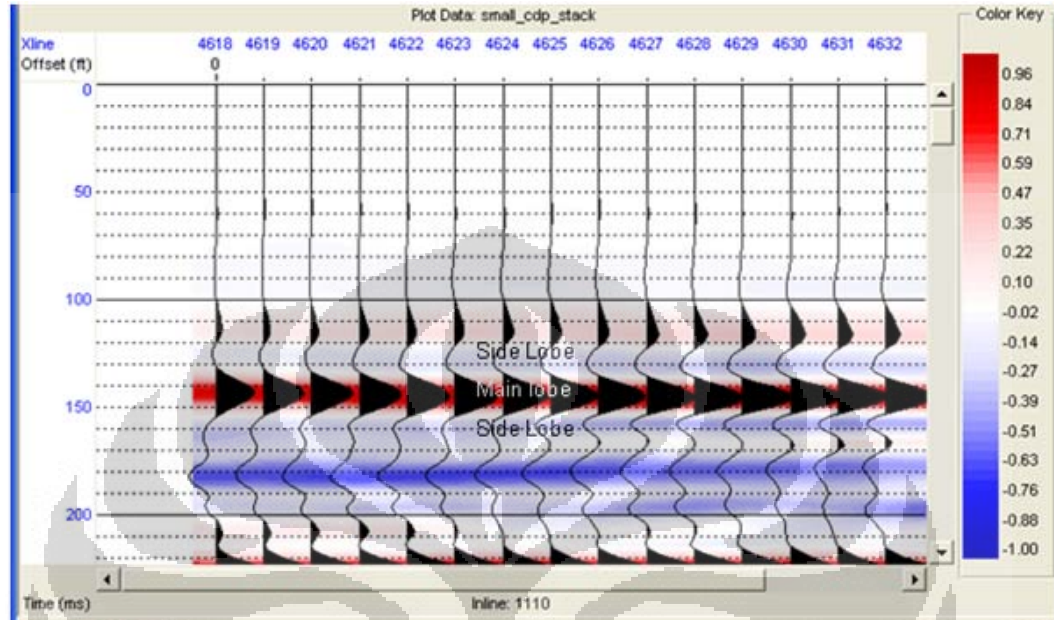


Figure 4.15. Determining the seismic polarity

4.3.3. Seismic Data Conditioning

The processing of Seismic Data can have a critical impact on the AVO Analysis. In this project, we apply the following process to the original NMO Corrected gathers (Figure 4.16). Figures are available in sequence.

- Trace Mute: to limit the influence of long offset traces, where the noise level is high.
- Super Gather: to reduce random noise while preserving offset-dependent amplitude variations.
- Bandpass Filter: to suppress noise.
- Radon 1st pass: in this case it was to remove the up-going events.
- Radon 2nd pass: to remove the down-going events.
- Trim Static: to align the traces.
- Angle Gather: creating Angle Gather to be used in the Simultaneous Inversion process.

Below are the Figures of the Seismic Data Conditioning and the parameters.

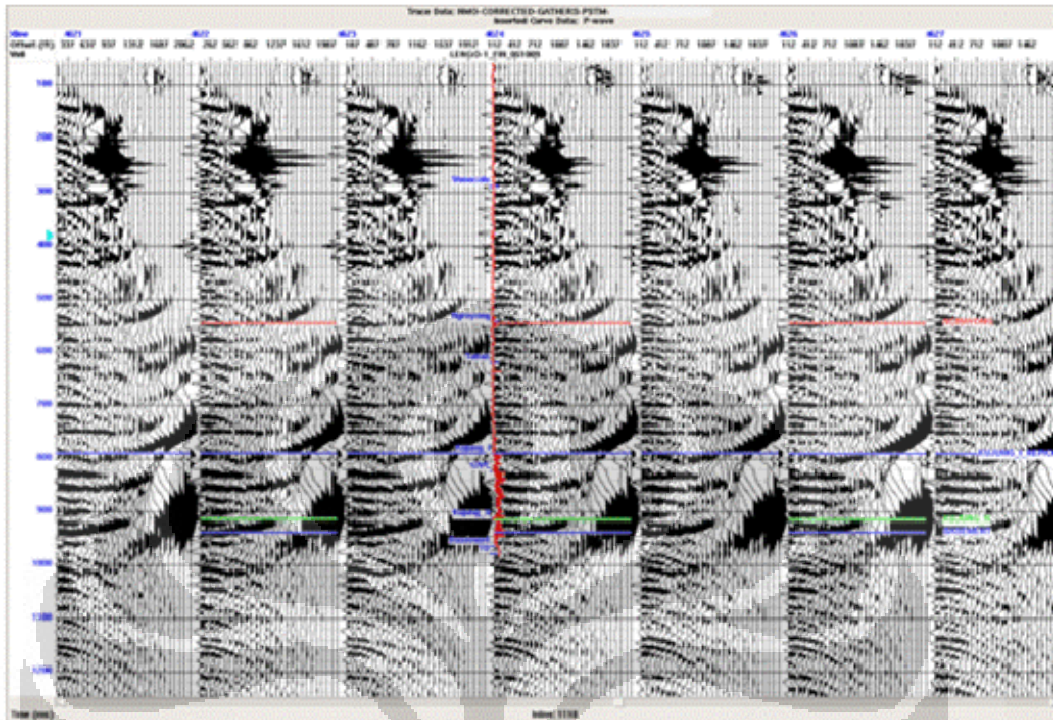


Figure 4.16. NMO Corrected Gathers

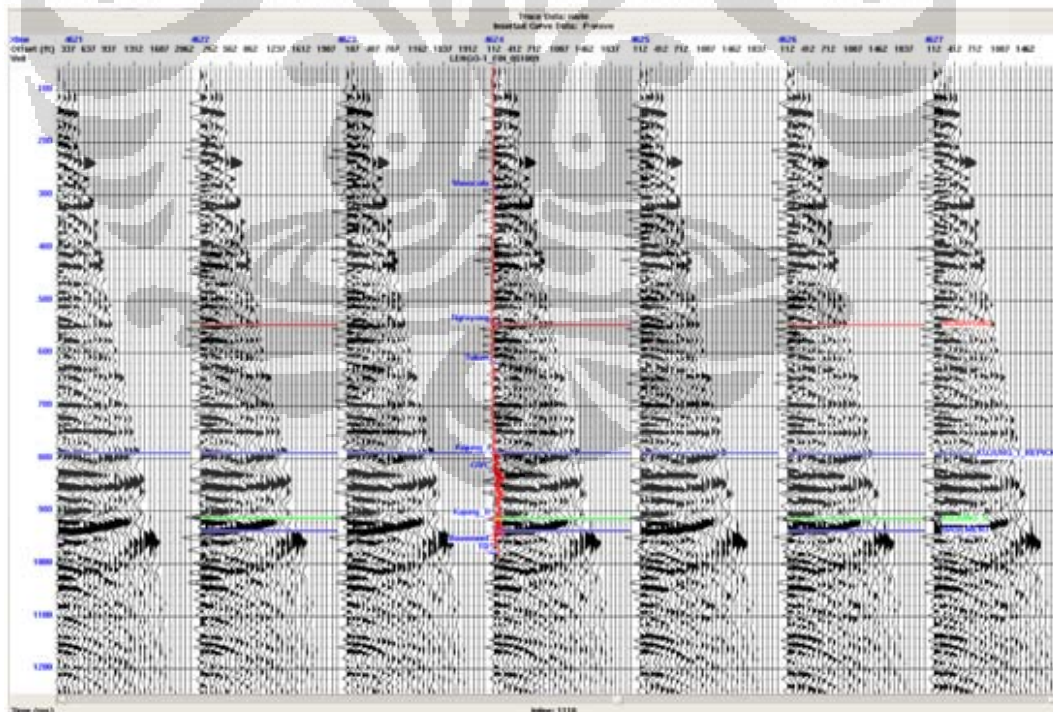


Figure 4.17. Trace Mute

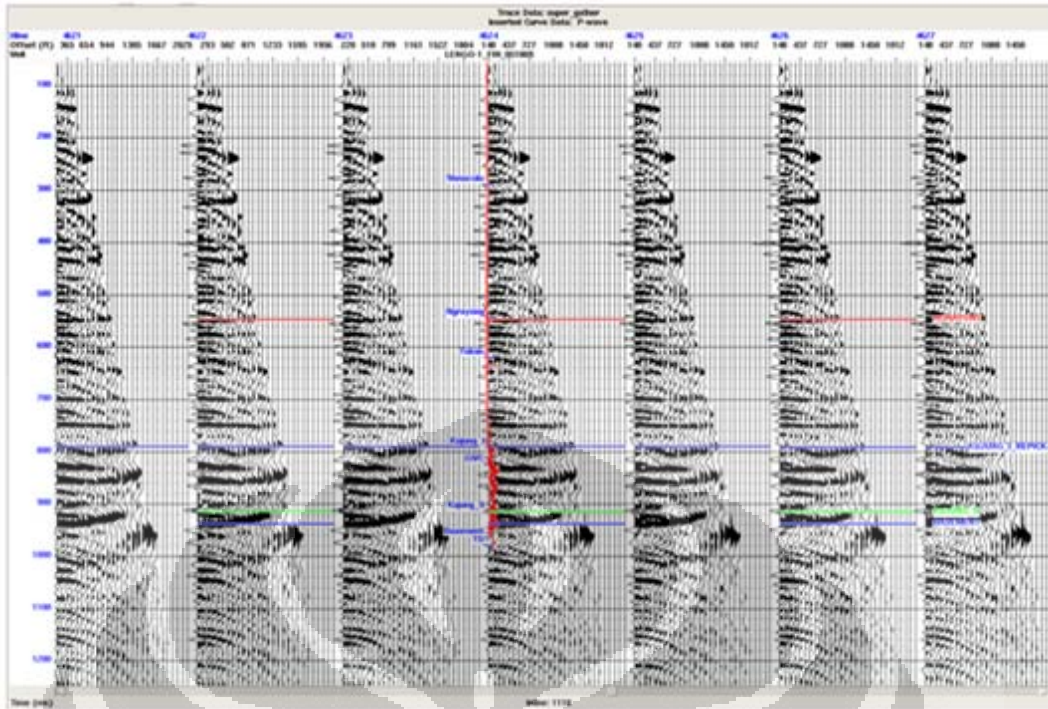


Figure 4.18. Super Gather

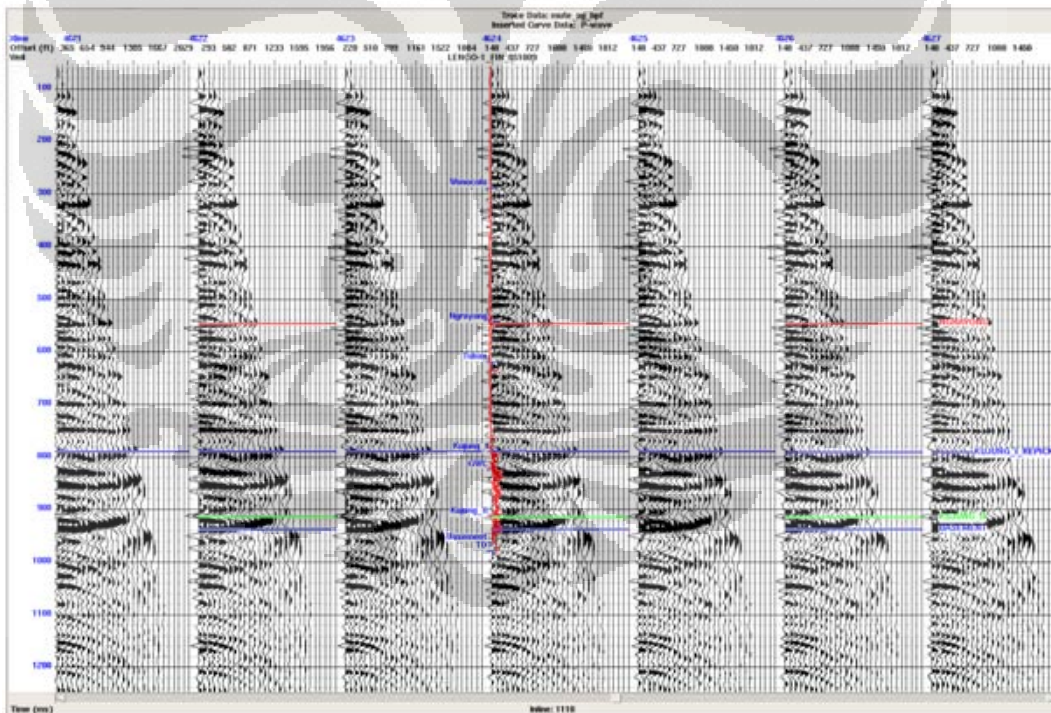


Figure 4.19. Bandpass Filter

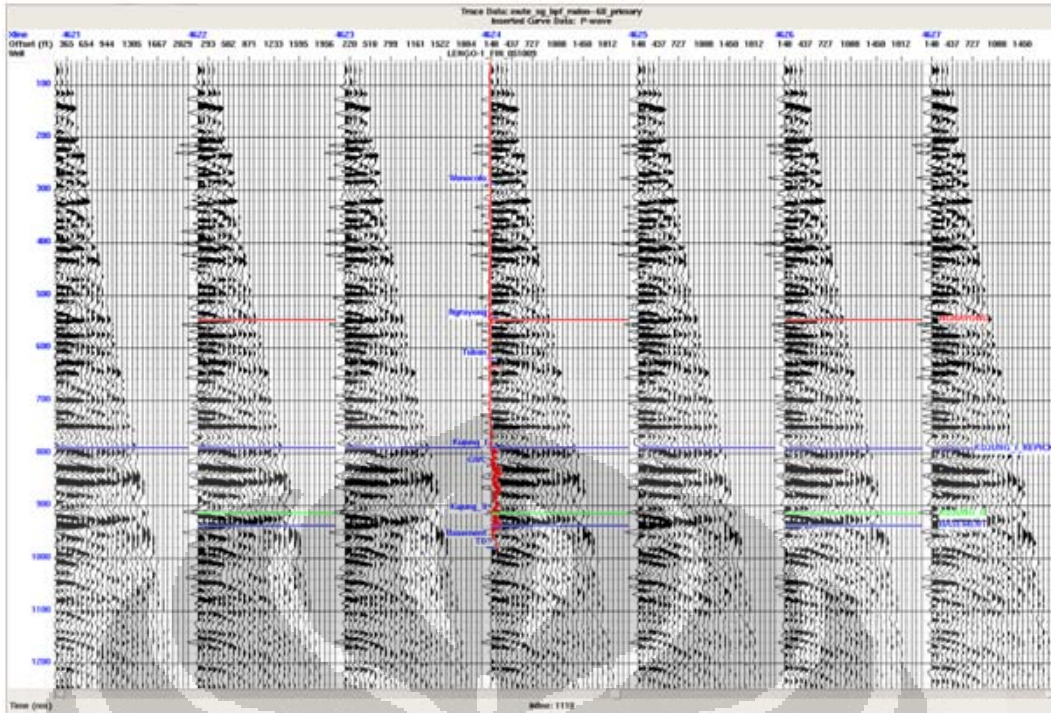


Figure 4.20. Radon 1st pass

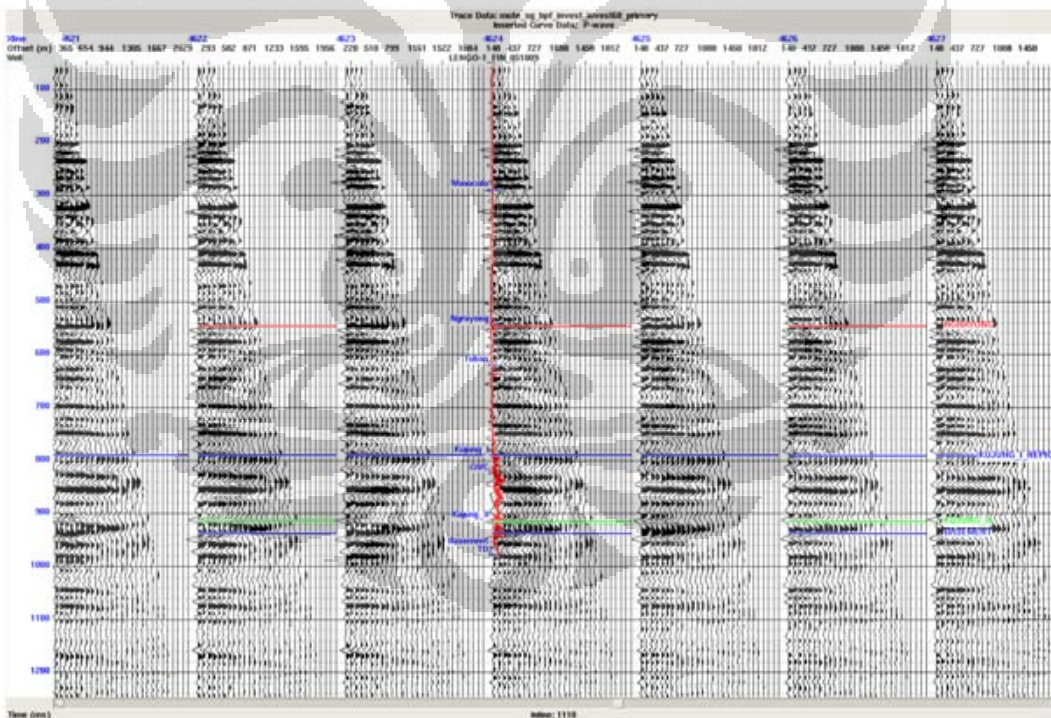


Figure 4.21. Radon 2nd pass

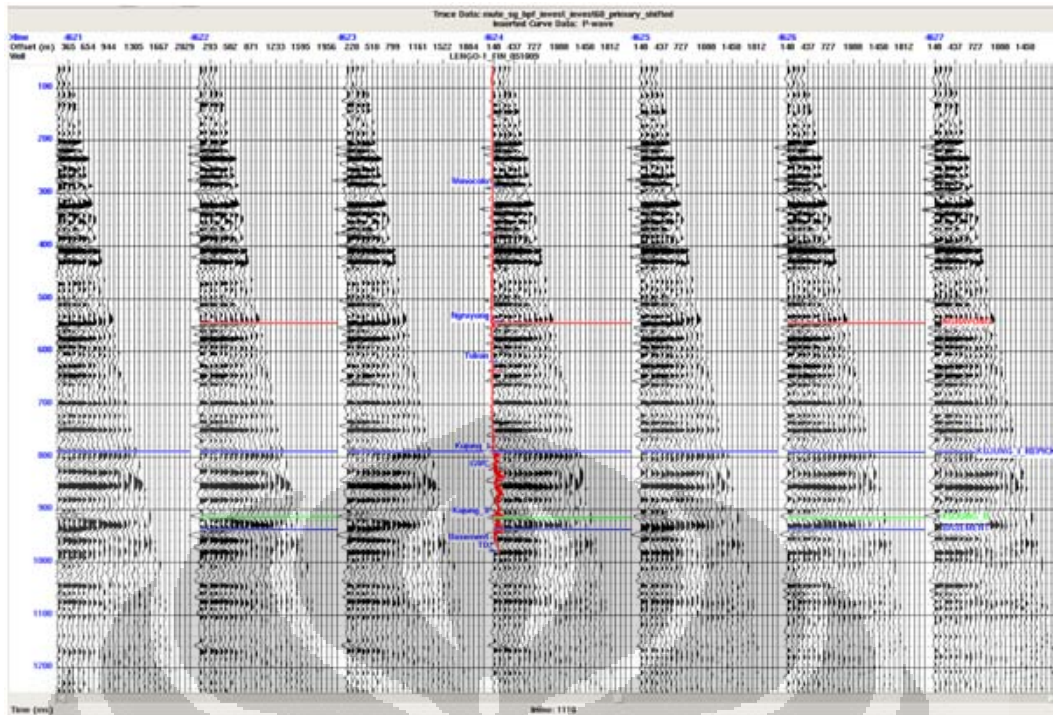


Figure 4.22. Trim Static

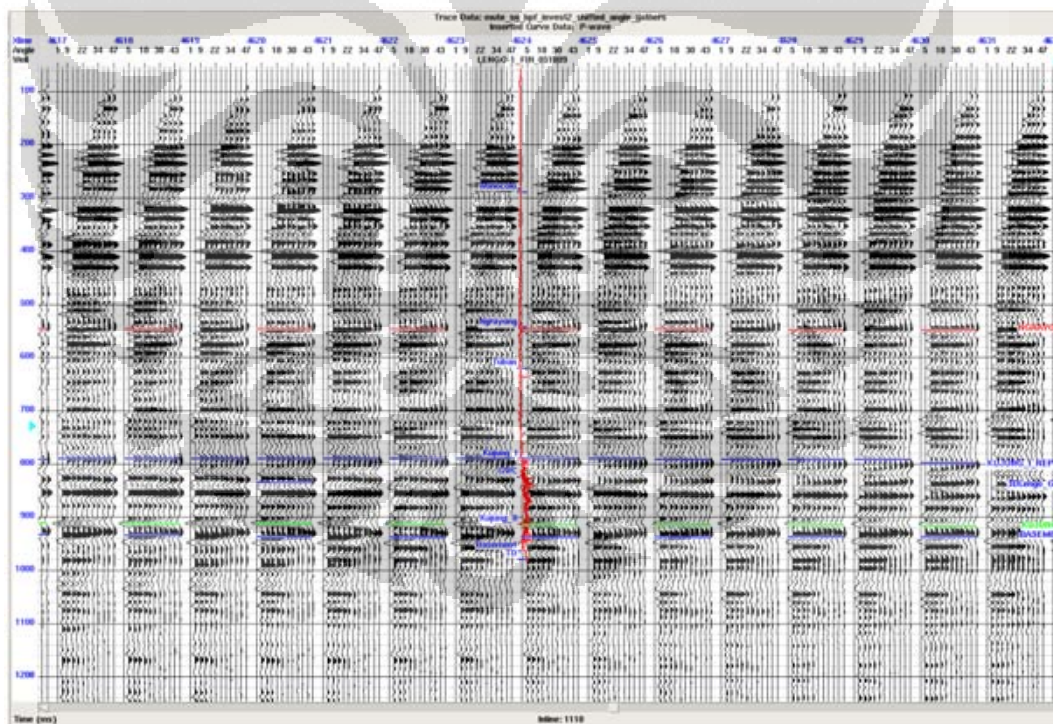


Figure 4.23. Angle Gather

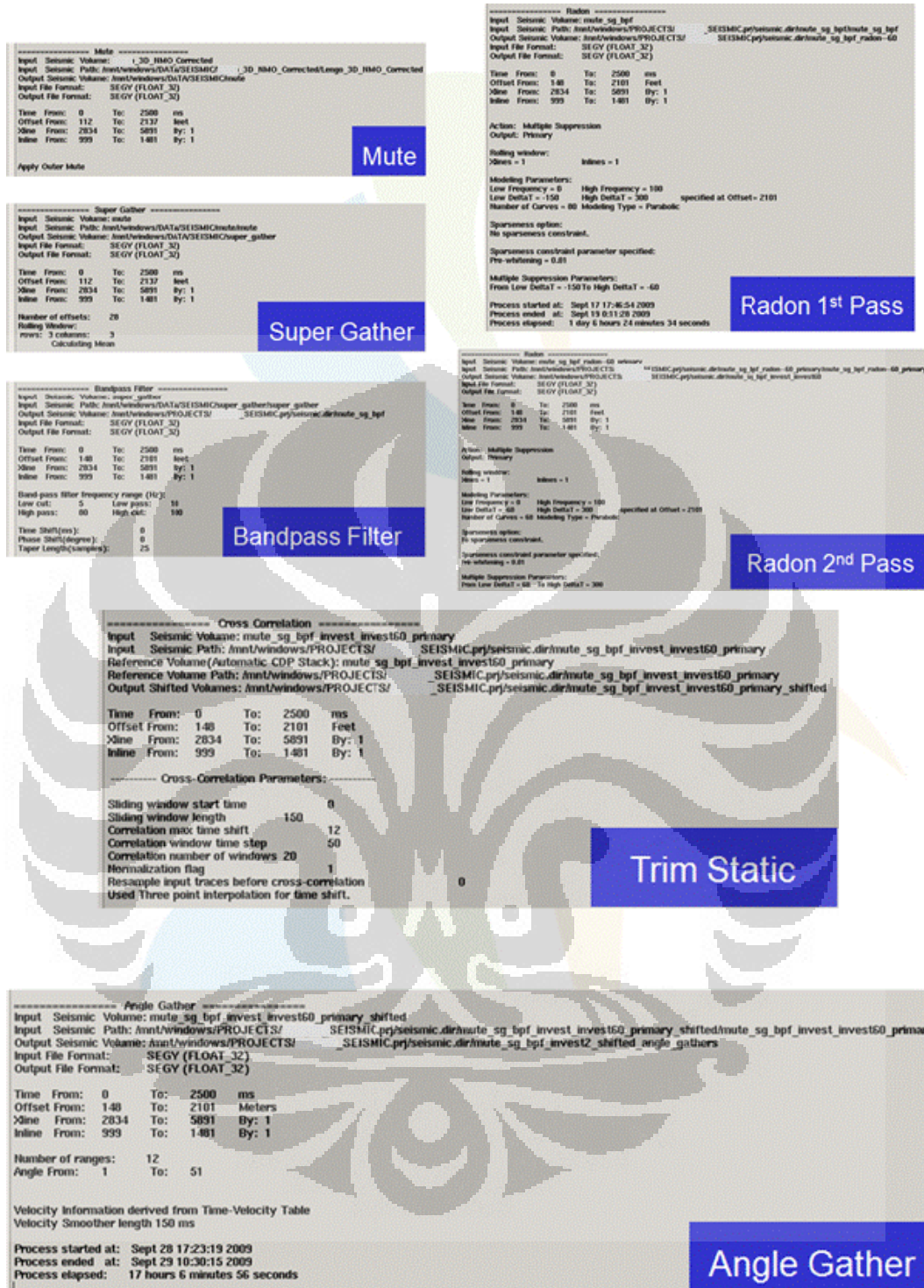


Figure 4.24. Seismic Conditioning Parameters

4.4. AVO ANALYSIS

The seismic gather at the well location was analyzed to determine the AVO characteristics.

The AVO characteristic for NGRAYONG and KUJUNG1 tops are similar: both are High Impedance events that dim with offset, typical of an AVO Class 1.

The NGRAYONG shows a strong AVO effect and lies far from the central data cluster.

The KUJUNG1 is much weaker.

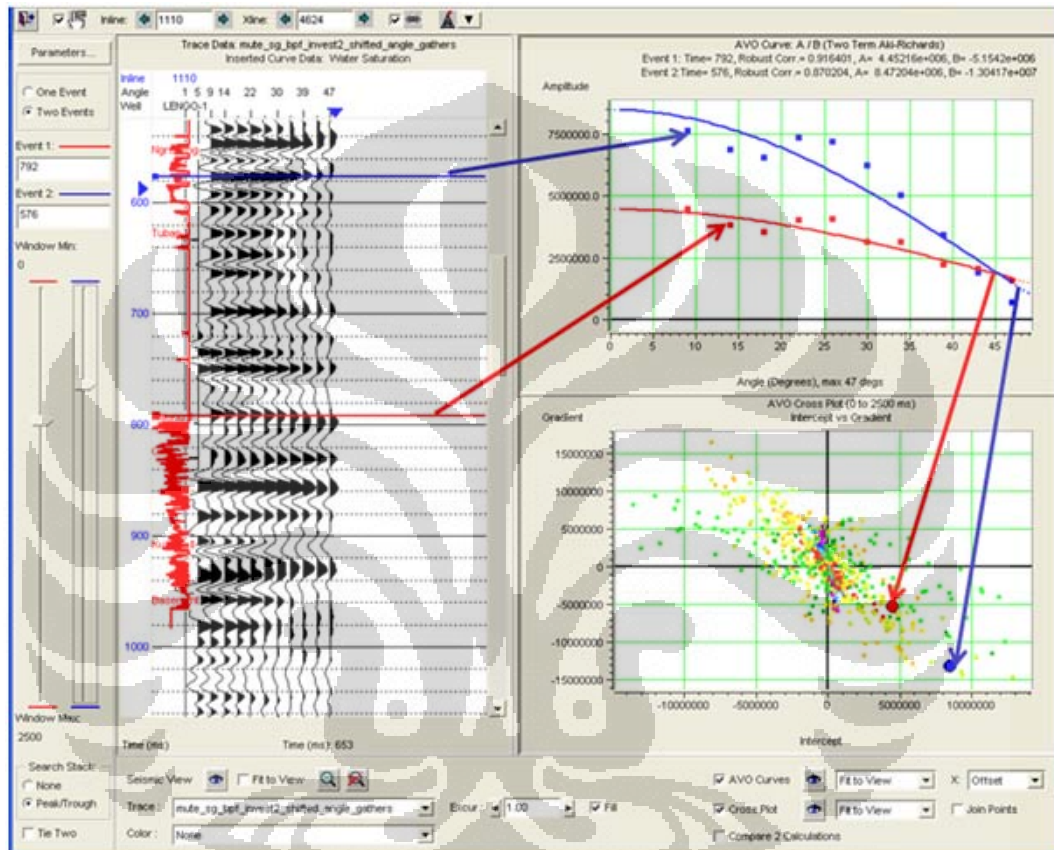


Figure 4.25. AVO Analysis

4.4.1. AVO Attribute Extractions

A simple summary of the theory for AVO volume extraction is that seismic data is normally collected at a number of different offsets between the source and the receiver. The collection of multiple traces for a common midpoint location is called an *offset gather*. Conventional seismic processing and interpretation assumes that the seismic data is collected at zero offset and so the offset gather is usually stacked into a single trace – since the stacking process is one of the best tools for improving the signal-to-noise ratio. However, the

amplitudes of a reflection event will vary with offset (or incidence angle). The amplitude difference with offset (or angle) is particularly strong in the reflection events associated with gas-charged sands. The reason for the change in amplitude with offset is due to a change in the *Poisson's ratio*, which is a measure of the V_p/V_s ratio. Compressional wave (V_p) velocities are particularly sensitive to the presence of gas whereas the shear wave (V_s) velocities are influenced by the lithology of the rock. In other words, the difference in the shear-wave velocity between a gas-charged and a wet reservoir is minimal whereas the difference in the compressional-wave velocity is very significant. Thus, the ratio of the V_p and the V_s velocities is a direct indicator of hydrocarbons and it can only be measured by comparing the traces at different incidence offsets (or angles). This type of analysis is termed *AVO* for *Amplitude versus Offset*. Since the analysis is actually performed in the angle domain, the term *AVA*, *Amplitude versus Angle*, is also used.

The change in the reflection amplitudes with a change in offset is a measure of the V_p/V_s ratio. Thus, the pre-stack gathers need to be analyzed and reduced to a more direct measurement of the V_p/V_s ratio. There are two common methods for data reduction of pre-stack gathers: the Intercept/Gradient (A/B) calculation and the V_p Reflectivity/ V_s Reflectivity (R_p/R_s) calculation. The Fluid Factor attribute is also a common pre-stack attribute and is formed from a combination of the R_p and R_s volumes.

The A/B calculation requires that the pre-stack gathers be transformed from the offset domain (i.e., the offset distance between source and receiver, measured in terms of meters or feet) to the angle domain (i.e., traces of common incidence angles). The transformation to the angle domain is done mathematically using a velocity function and the Dix approximation. The angles are transformed to sine-squared ($\sin^2 \theta$) and plotted versus the amplitudes. A linear regression fit is then made through the data points: the intercept of the line with 0-degree angle is termed the Intercept (or A) and the slope of the line is the Gradient (or B).

For NSH Field, the AVO Attributes were extracted from the Angle Gathers using a two term reflectivity approximation, allowing for extraction of the Intercept, A, and the Gradient, B.

For an AVO Class 1, we expect that the Intercept and Gradient would be of opposite sign. Also, we would expect the Gradient to be stronger in areas that have hydrocarbons.

The Attribute below is the Gradient*sign(Intercept). The Top and Base of a Class 1 AVO Anomaly should both be a strong negative.

A number of anomalies in the NGRAYONG coincide with the AVO Attributes. They are lacking in the KUJUNG1, but they also seem to be present in the KUJUNG2.

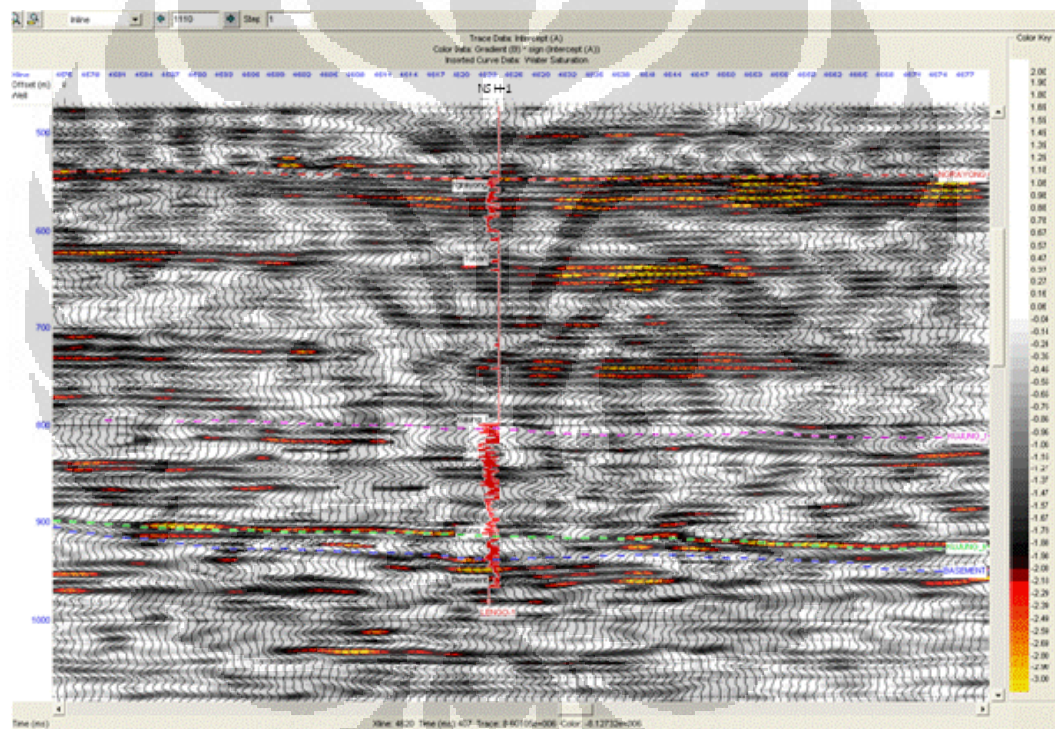


Figure 4.26. AVO Attribute showing Gradient*sign(Intercept)

4.5. SIMULTANEOUS INVERSION

The inversion process is an attempt to convert the seismic wiggle trace into a series of layers that represent the geology. Seismologists think of the seismic trace as a series of spikes, caused by contrasts in the P-impedance, which are convolved with a wavelet generated by a seismic source. This is called the forward model. Going backwards in the model is called *inversion*. Inversion, in

the case of exploration seismology, is the idea that the seismic traces and the wavelet are known, and so we can deconvolve the seismic data to yield the series of spikes (or layers) that created the trace. However, the inversion process suffers from a condition known as *non-uniqueness*: there is an infinite set of possible geological layer solutions that can provide the same seismic trace. The non-uniqueness issue is generally handled by adding *a priori* information. One piece of information that is commonly added is the low frequency trend of the geology. The low frequency information is added by creating a model of the geology using existing wells and the seismic horizons. The other piece of information that is added to the solution is by adding constraints, for example, constraining how far the inversion result deviates from the initial model.

Traditionally, seismic inversion operated on a single post-stack seismic trace. Simultaneous Inversion, on the other hand, operates on the traces in a pre-stack gather. The benefits of this method of inversion are that the pre-stack gathers allow us to add further constraints to the solution. The constraint that is added is that the variation of the amplitudes with angle due to AVO effects can be incorporated. As discussed in the previous section, the AVO effects are a measure of the V_p/V_s ratio. The output to simultaneous inversion is not only the P-impedance but also the S-impedance data. By dividing the P-impedance data with the S-impedance data, the density terms cancel out and a measure of the V_p/V_s is obtained.

In practical terms, Simultaneous Inversion requires that the pre-stack gathers be in the angle domain.

4.5.1. Initial Model Construction & Inversion Parameter Testing

In this project, the angle gathers we created in the previous AVO work, had been flattened.

A single global wavelet from the correlation work had also previously been extracted during the well-to-seismic correlation. Simultaneous Inversion also requires a starting P-impedance and S-impedance model. These models were created using the NSH-1 well and the P-wave, Density and S-wave logs and interpolated using the Kujung 1 horizon (10/15 Hz filter was used). The initial model was then merged with the RMS velocity provided.

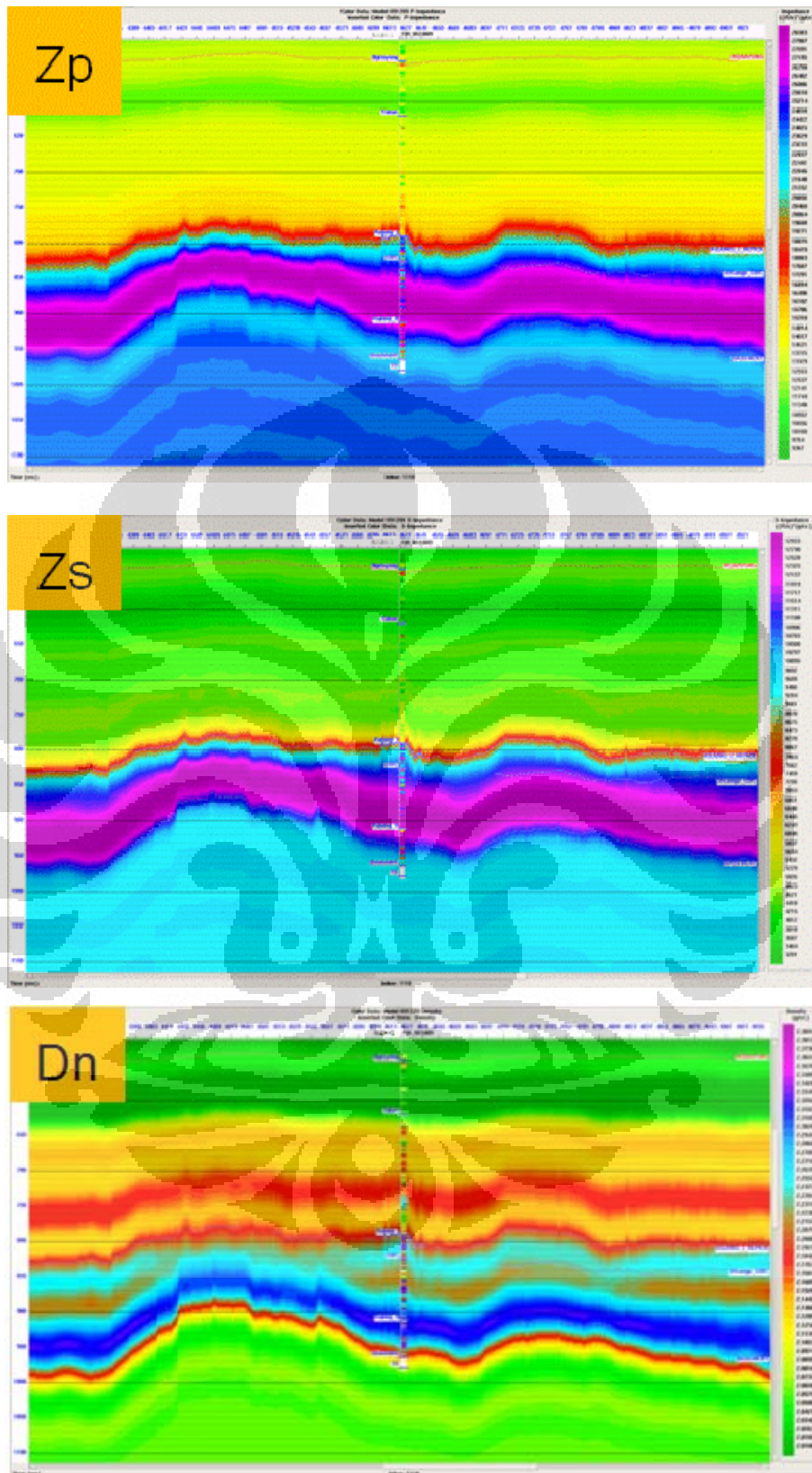


Figure 4. 27. Initial Model of Z_p , Z_s and Density, built using NSH-1 Well logs

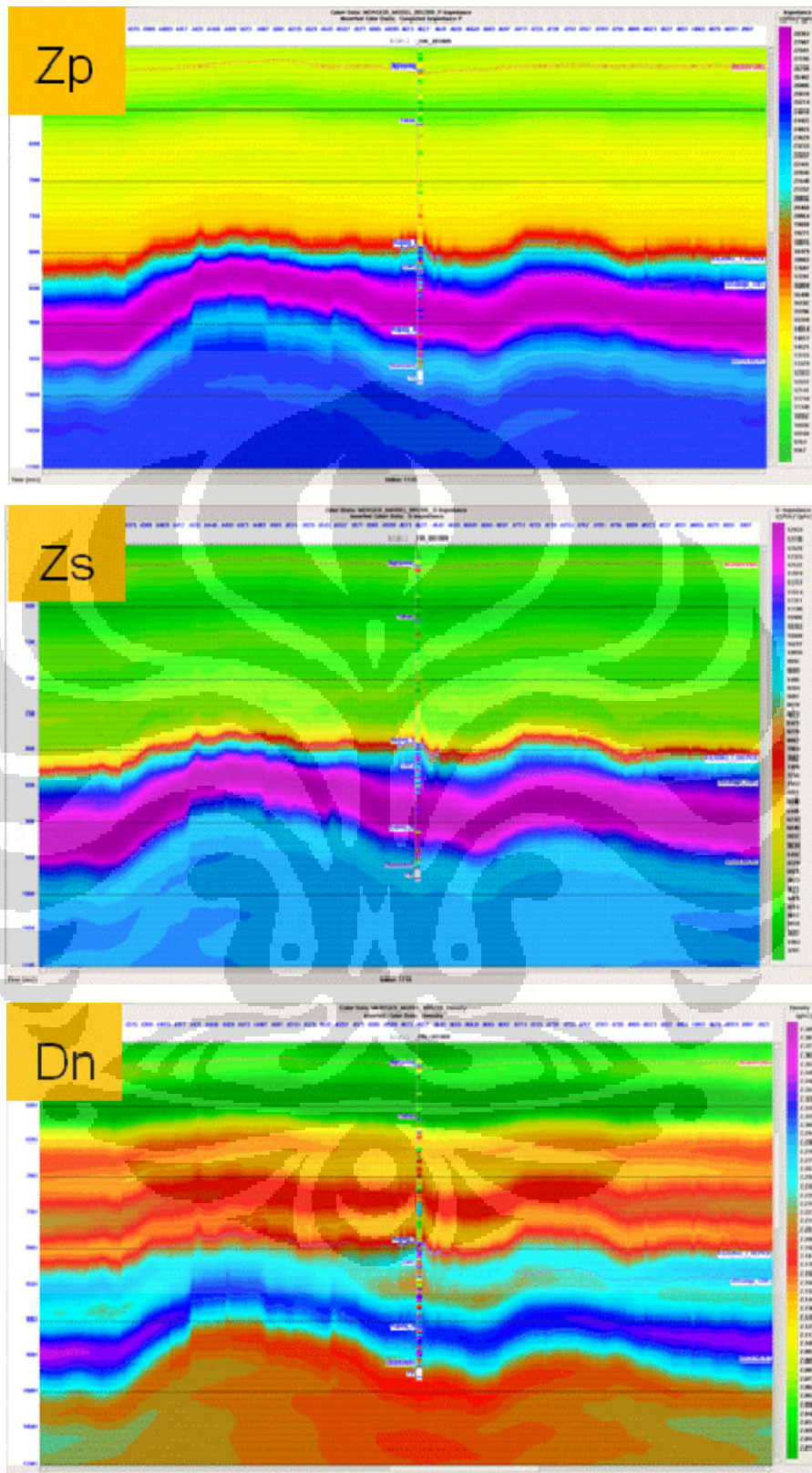


Figure 4.28. Initial Model of Z_p , Z_s and Density, built using NSH-1 Well logs and then merged with the RMS Velocity

A further constraint is required in the HRS software that relates the P-wave and the S-wave velocities for the wet background trend. As well, the regression between the P-wave and the density data is required. The regressions were measured calculated from previous work done with the NSH-1 well.

The computed regressions were done in the natural logarithm domain and they are as follows:

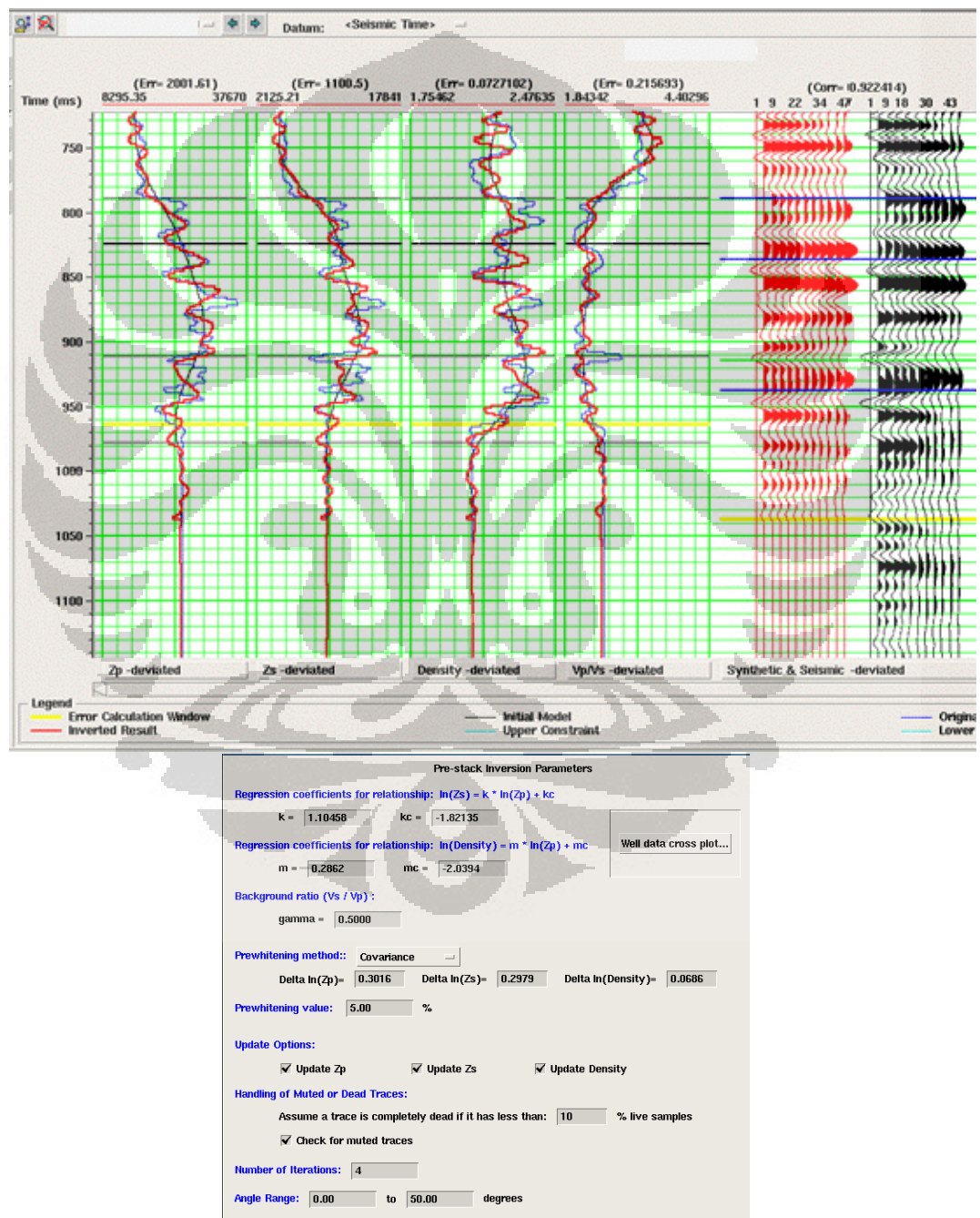


Figure 4. 29. Inversion Parameter Testing (pre-stack Inversion Analysis)

4.5.2. Simultaneous Inversion

Having chosen Inversion parameters that yielded the best fit of the inversion to the actual log measurements of Z_p , Z_s , Density and V_p/V_s , as well as yielding a good fit between the synthetic and the actual seismic gathers, the Simultaneous Inversion process was performed for the window of KUJUNG1 – 300 ms to BASEMENT +100 ms.

Below are the results of the Simultaneous Inversion Process: Z_p , Z_s , D_n , and V_p/V_s Ratio volumes.

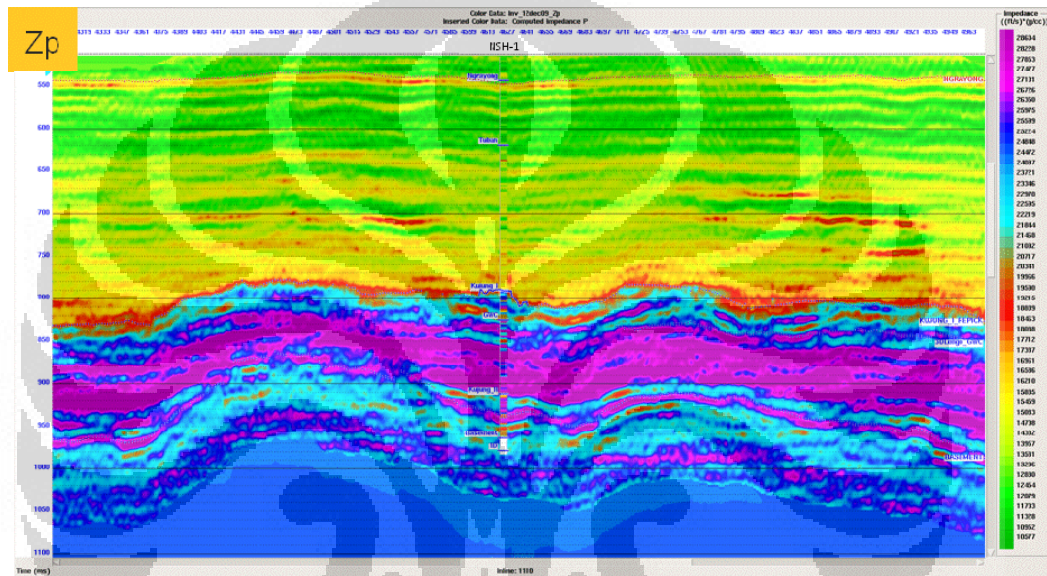


Figure 4. 30. Z_p volume

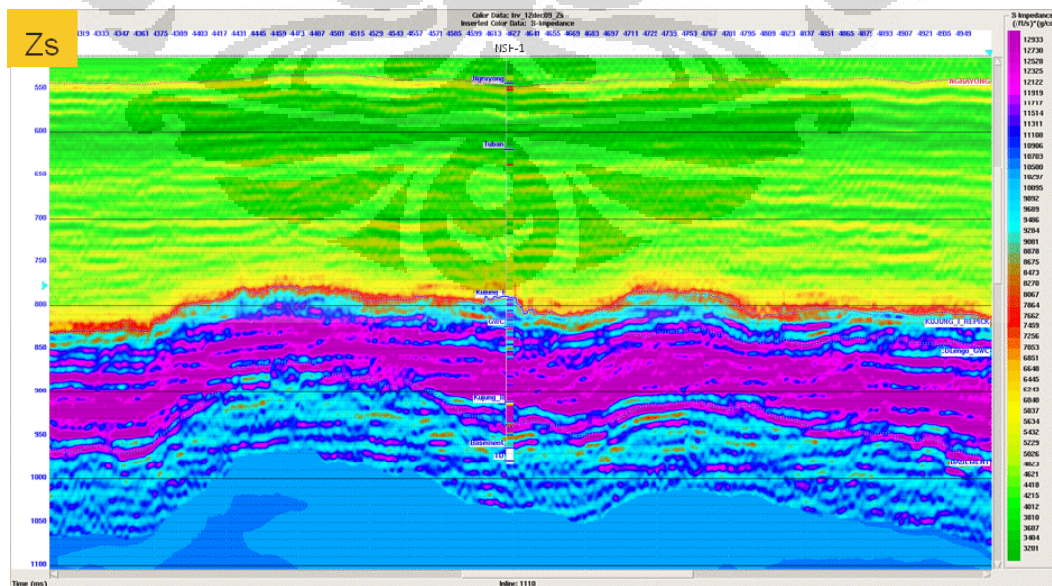


Figure 4. 31. Z_s volume

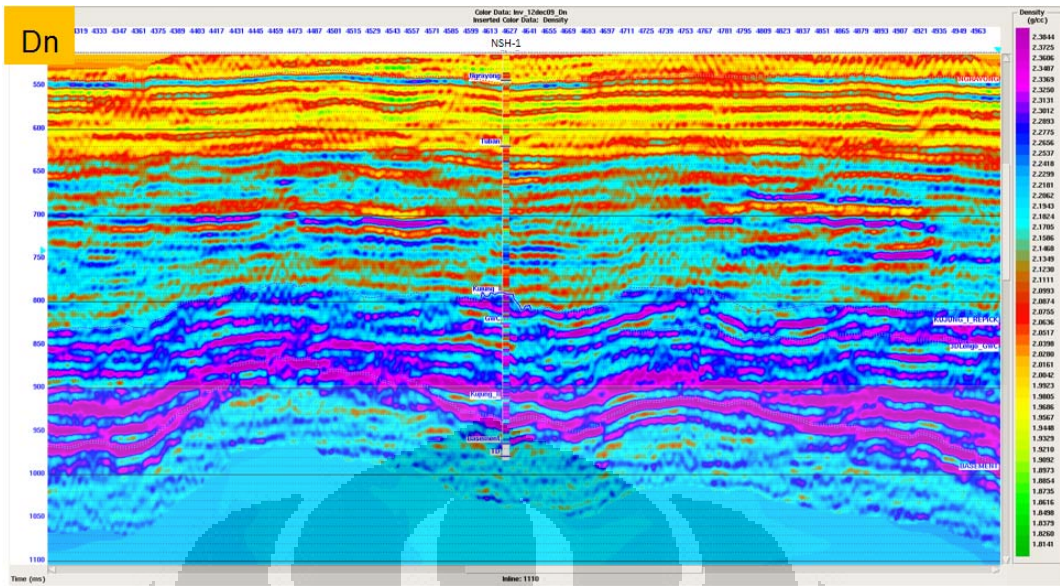


Figure 4.32. Dn volume

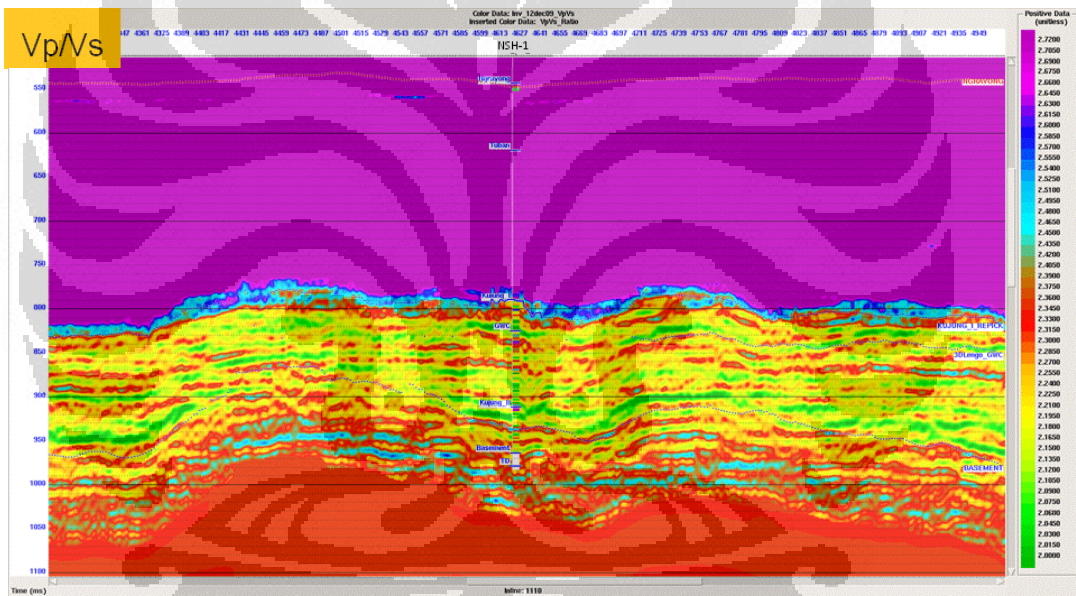


Figure 4.33. Vp/Vs ratio volume

4.5.3. Interpretation and Cross-plotting

Slices of Z_p , Z_s , and V_p/V_s Ratio were created by extracting Mean of the volumes from a 25 ms window below the Kujung1.

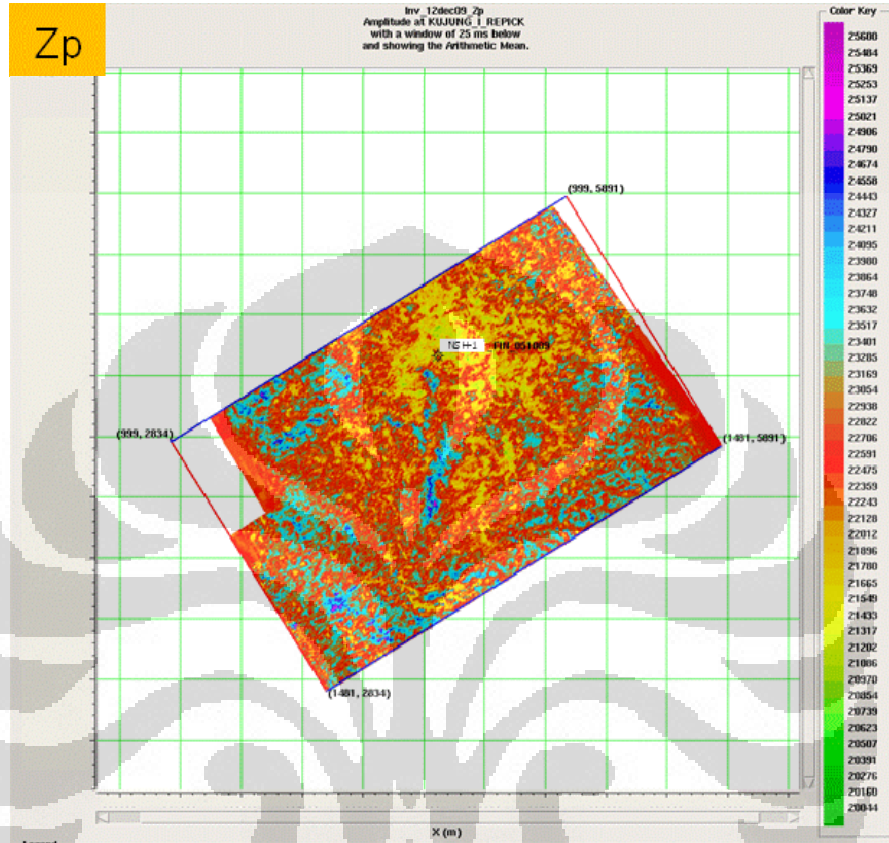


Figure 4. 34. Slice of Z_p , showing Mean of P-Impedance from a 25 ms window below Kujung 1

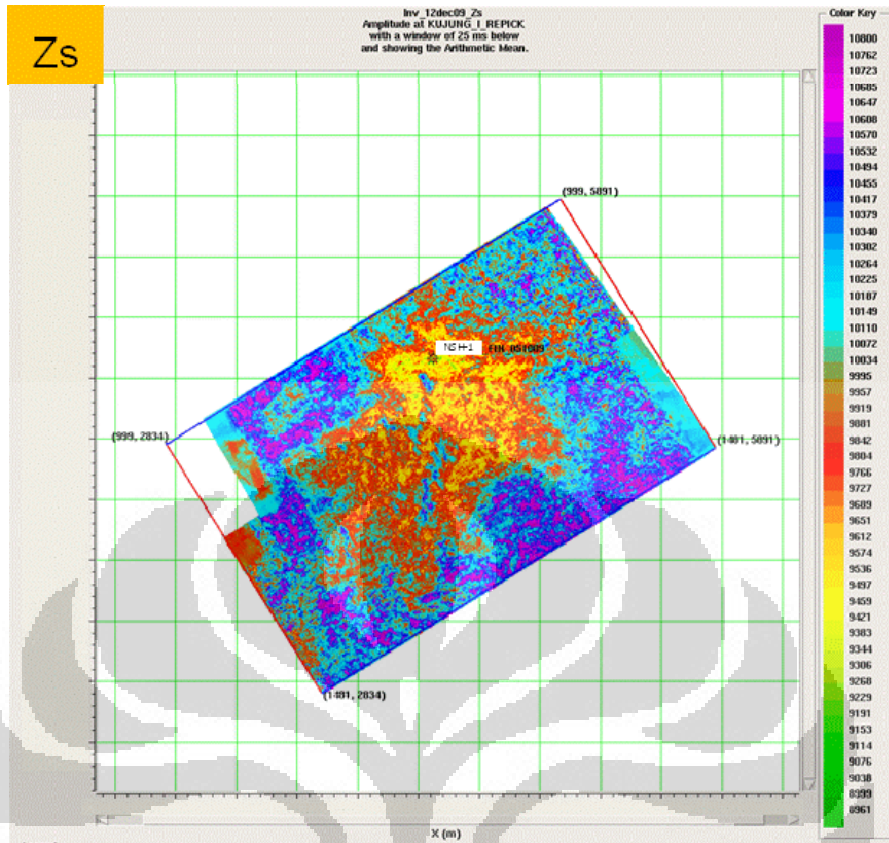


Figure 4.35. Slice of Zs, showing Mean of S-Impedance from a 25 ms window below Kujung 1

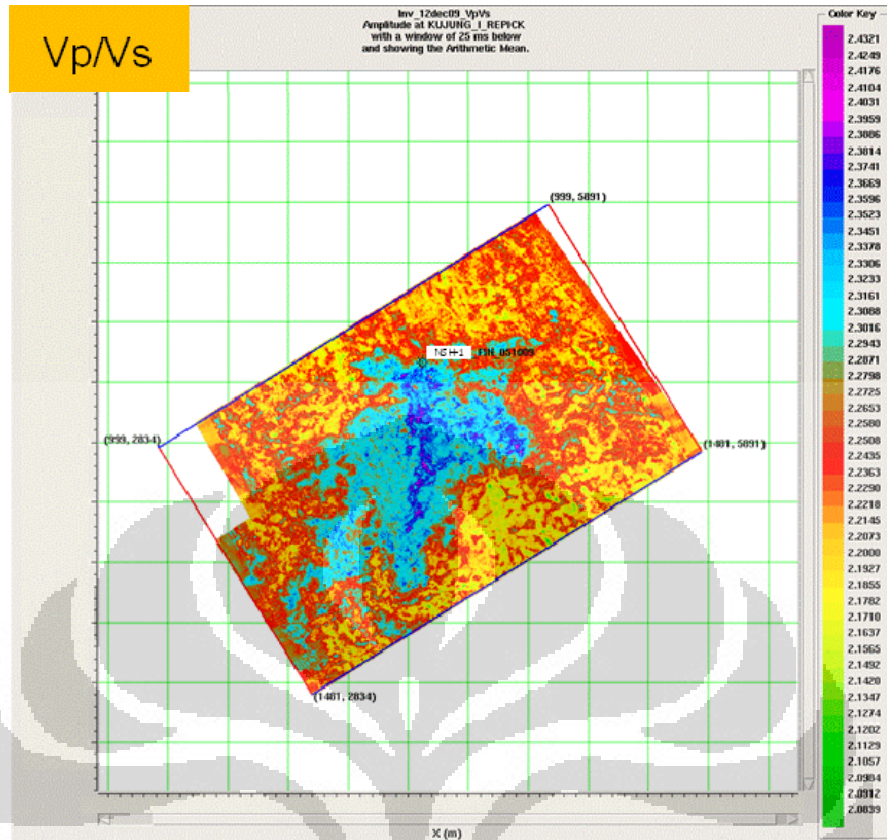


Figure 4.36. Slice of V_p/V_s , showing Mean of V_p/V_s from a 25 ms window below Kujung 1

After volumes of the Z_p and Z_s been computed, the interpretation of the results was undertaken by cross-plotting well logs and visually identifying the anomaly. Zones on the well log cross-plots that are thought as anomaly could be identified.

Later, the corresponding Impedance volumes could similarly be collected and the similar cross-plot is performed. Projecting the zones from well logs cross-plot and from the Impedance volumes cross-plot, similar trend is seen. Slice of the cross-plot zone is then created.

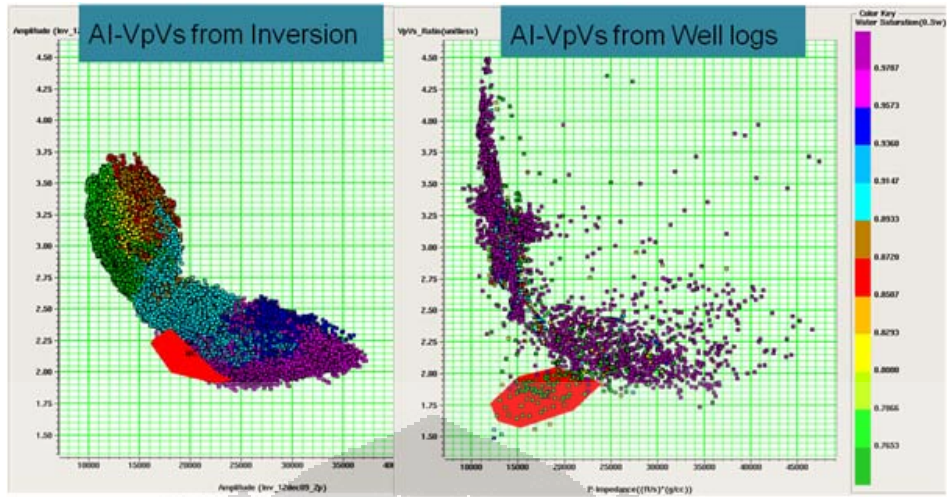


Figure 4.37. Cross-plot of AI vs VpVs from Inversion and from Well Logs

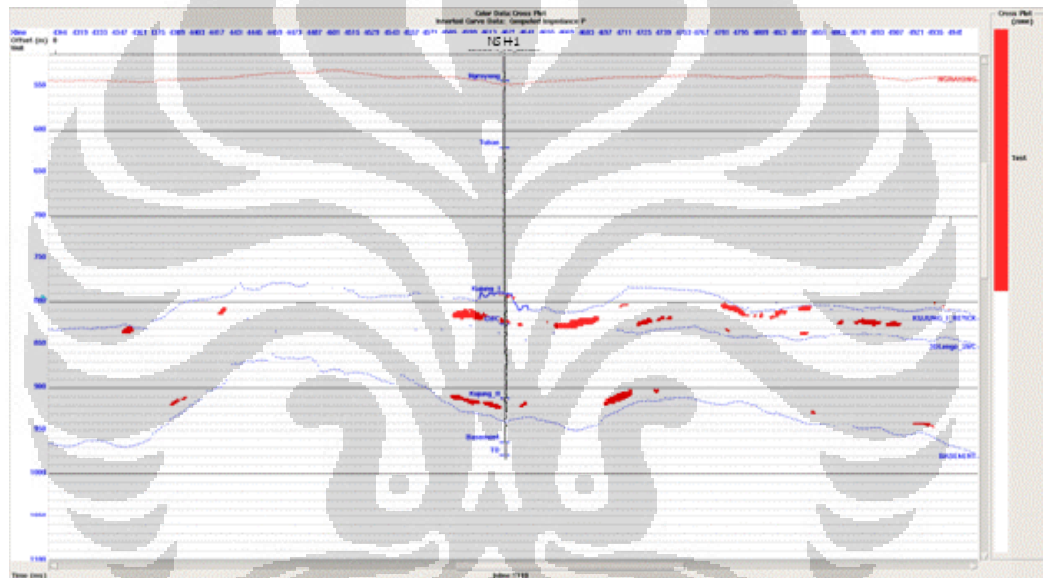


Figure 4.38. The projected zone from AI-VpVs from Inversion cross-plot

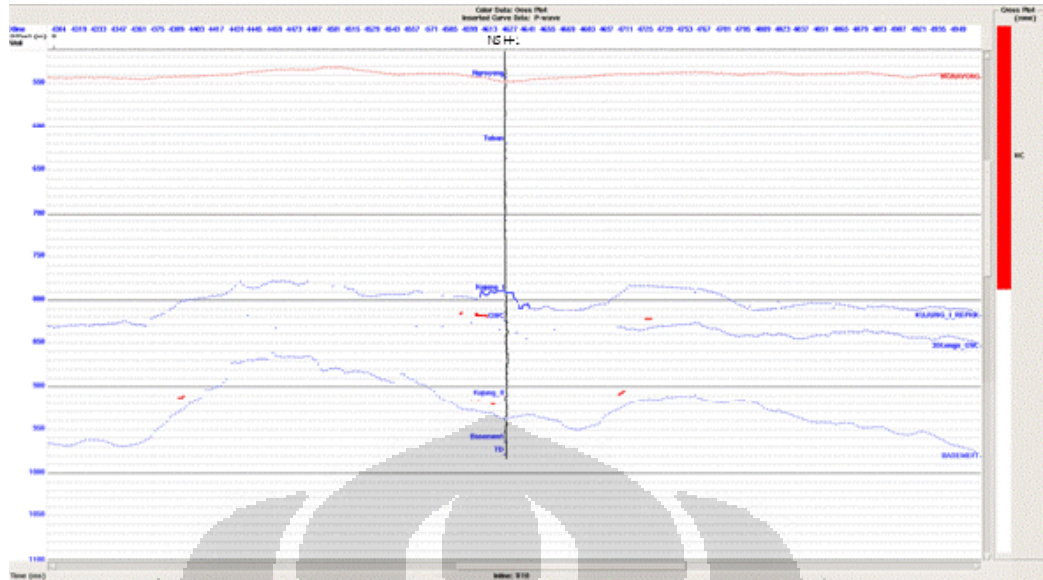


Figure 4.39. The projected zone from AI-VpVs from Well log cross-plot

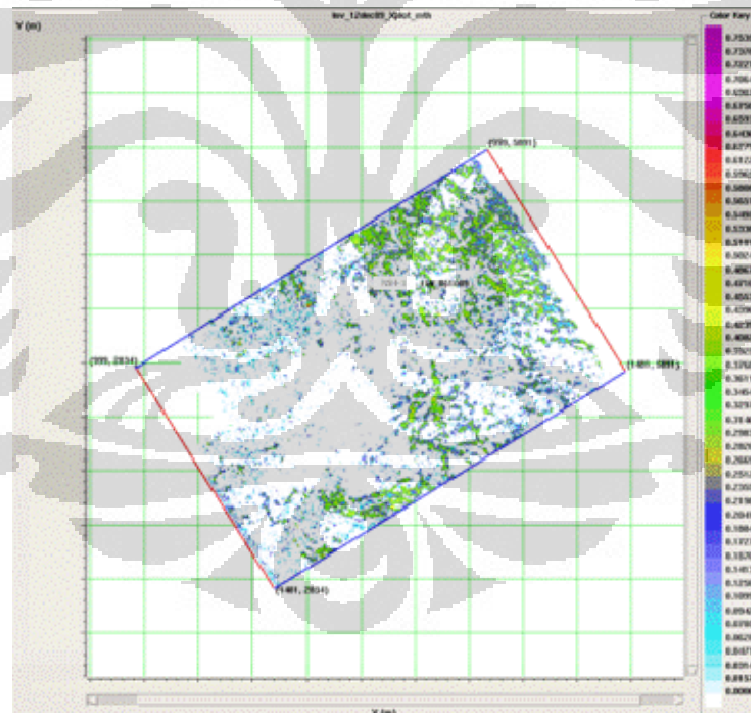


Figure 3. 40. Slice of the Cross plot zone

4.5.4. LMR: Interpretation and Cross-plotting

After the P-Impedance and S-Impedance volumes had been generated, a mathematical transformation can be applied to the two volumes to generate what are known as Lambda-Rho and Mu-Rho volumes. The significance of these

volumes is that, when cross-plotted, the gas and other lithologies can be more easily distinguished.

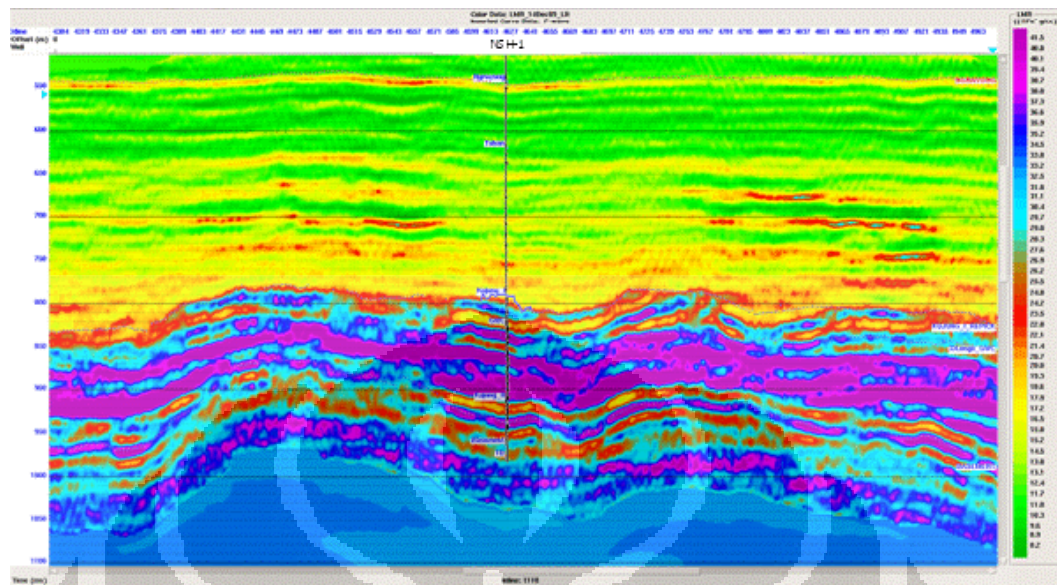


Figure 4.41. Lambda-Rho Volume

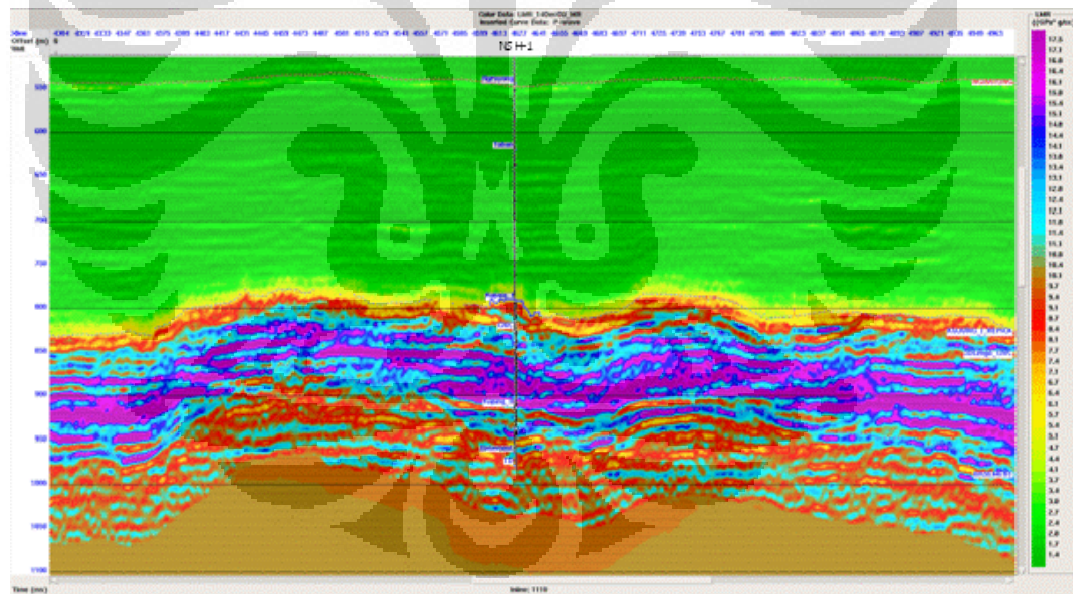


Figure 4.42. Mu-Rho Volume

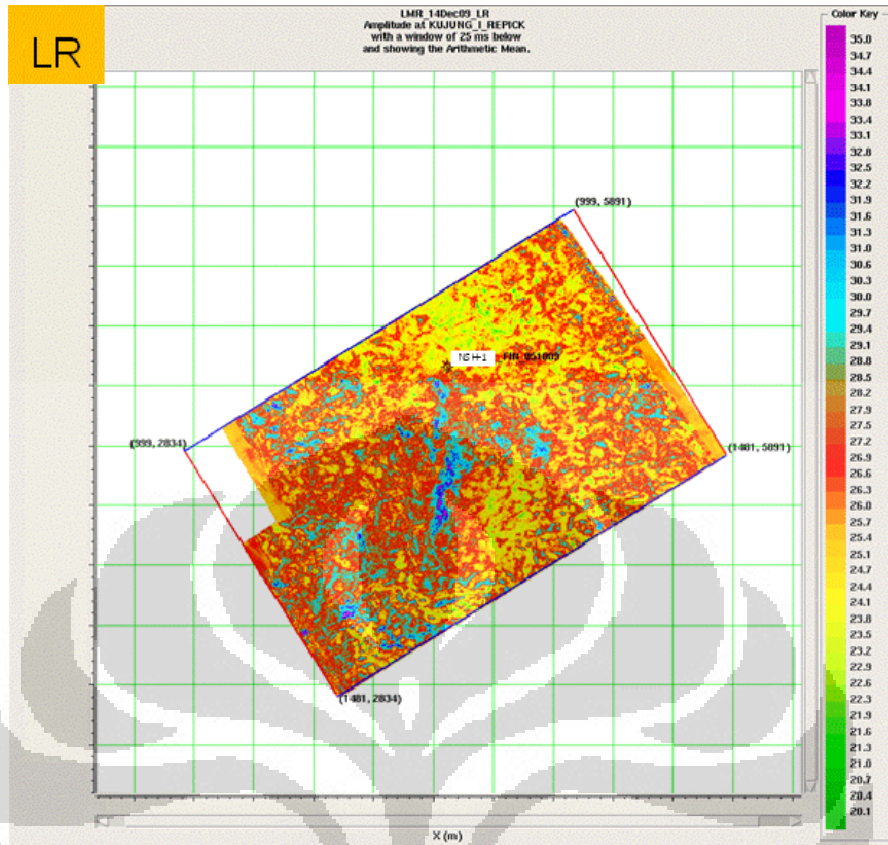


Figure 4.43. Slice of Lambda-Rho Volume

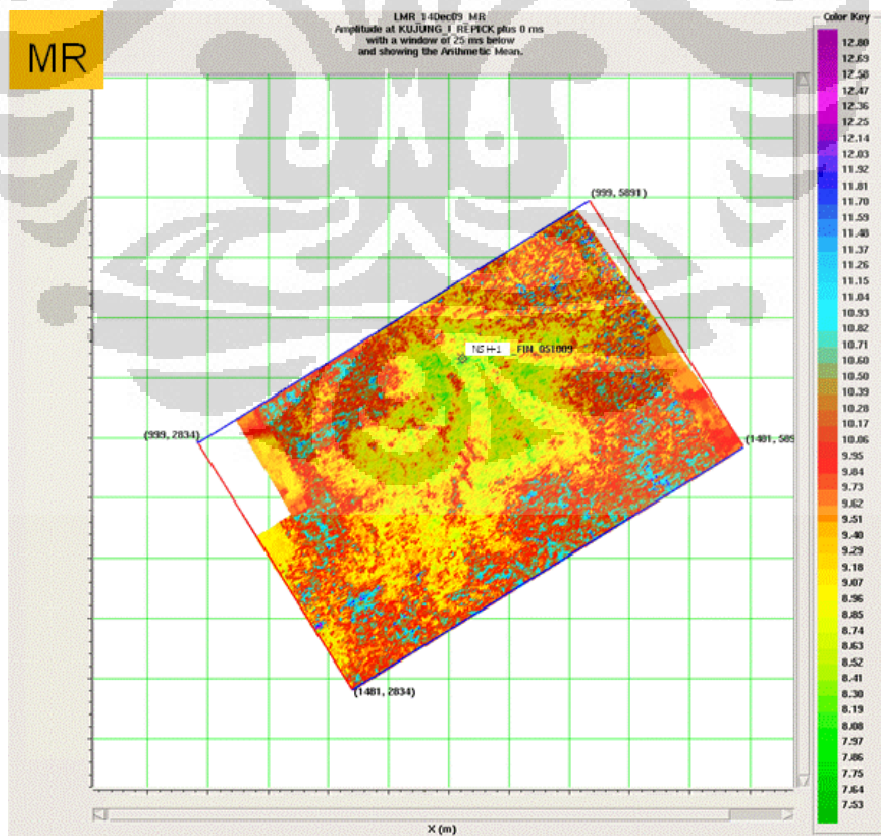


Figure 4.44. Slice of Mu-Rho Volume

Similar with the Inversion result, we can crossplot the LMR logs, predict the anomaly zones and post the zone in the LMR Volumes cross-plot. Projecting the zone onto the LMR volumes, again, similar trend is seen.

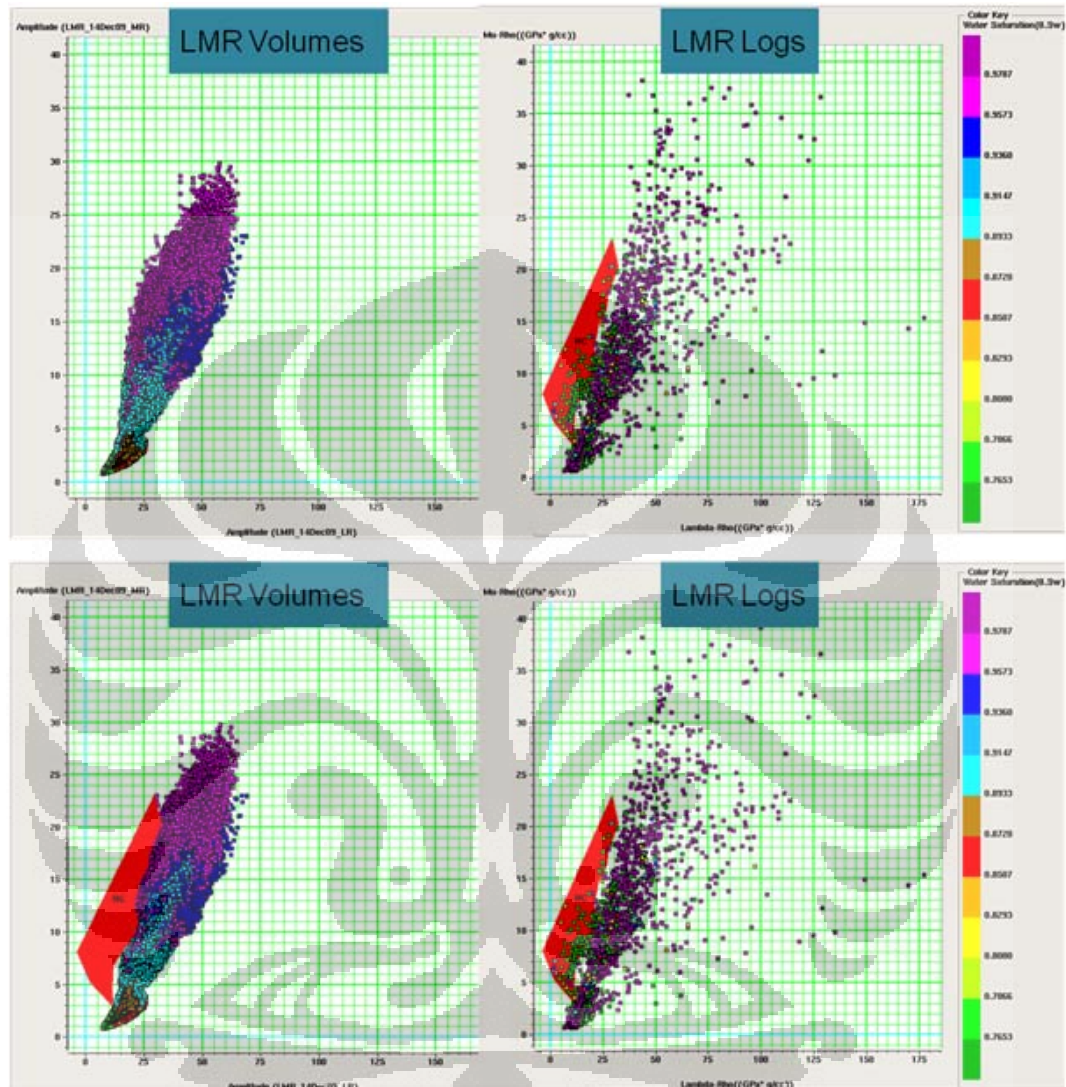


Figure 4.45. Cross-plot of LR vs MR from LMR Volumes and from Well Logs

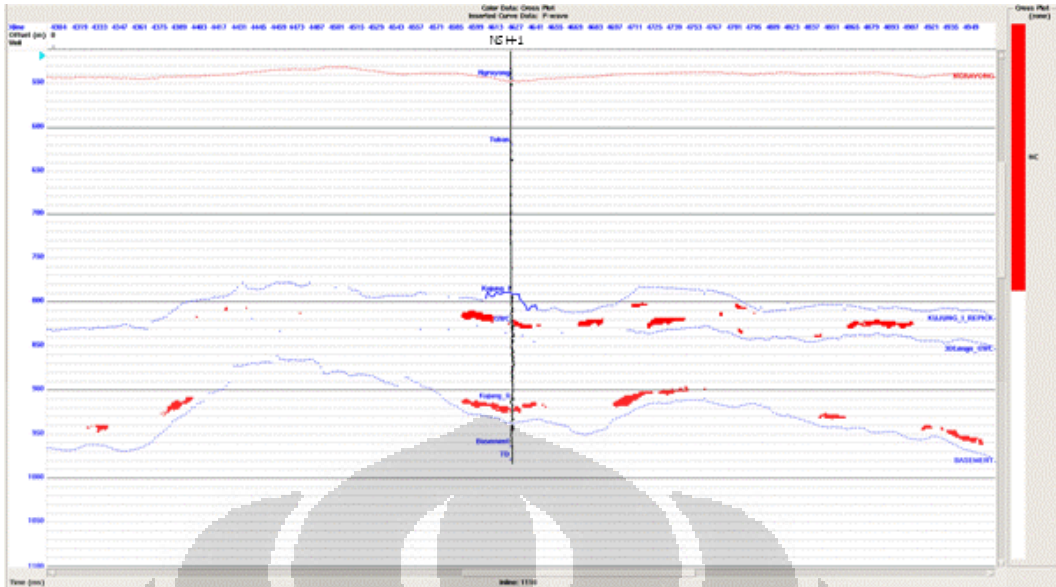


Figure 4.46. Projected zones from LMR Volumes

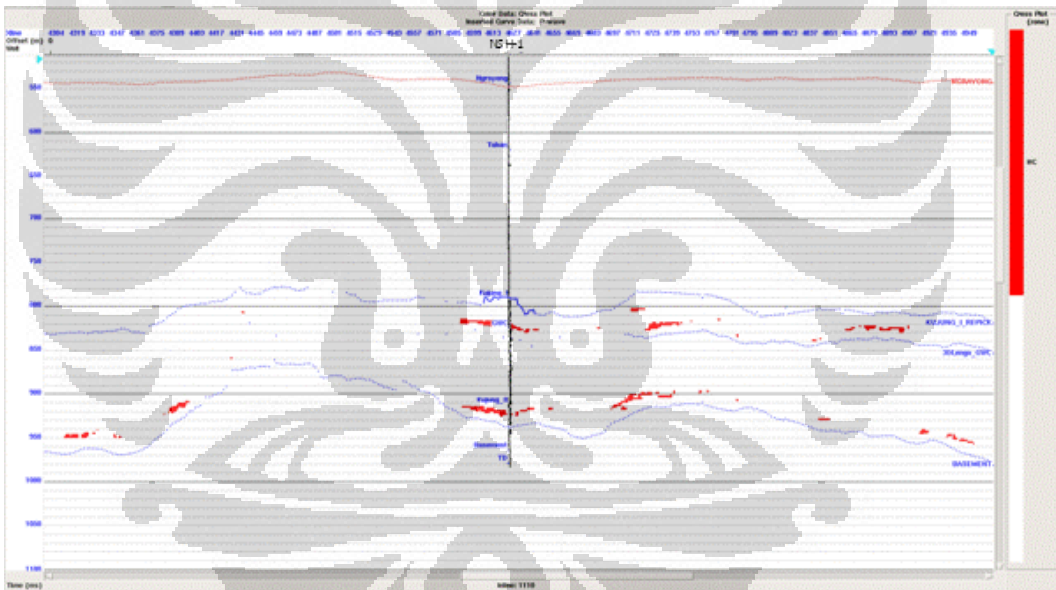


Figure 4.47. Projected zones from LMR logs cross plot

CHAPTER V

CONCLUSIONS AND RECOMMENDATIONS

Conclusions and recommendations for this thesis are :

1. Extracting fluid information from seismic data in carbonates is very difficult. There are seismic imaging issues due to interbed multiples, anisotropy, fractures and voids that cause problem to the seismic signal and are difficult to remove using even the best seismic processing practices and algorithms.
2. However the near offset traces are generally good enough to yield a good image of the P-Impedance reflectivity which is strongly linked to the porosity.
3. In this case, it is believed that the P-Impedance inversion results are more reliable indicators of porosity and that the interpreted fluid effects should be treated with caution.
4. The LMR logs were initially created to highlight errors in the velocity logs (if there's any). When cross-plotted, the LMR logs are then used to show area that are interpreted as HC anomaly which has the value between 3 – 20 GPa*gr/cc for Mu-Rho and below 20 GPa*gr/cc for Lambda-Rho.
5. Wavelet is known to have maximum impact to the inversion result. Testing and comparing the inversion result when using single wavelet and angle-dependent wavelet gave no significant difference.
6. The AVO analysis in this study was not show the good quality in carbonate, because the AVO used for sandstone reservoir, but for LMR method, it could distinguished the HC anomaly
7. Recommendations:
 - a. consider the possibility to investigate PSDM to improve seismic quality
 - b. Test Bayesian litho-classification on the inverted volumes. By doing this, one would be able to quantify the uncertainty associated with classifications.

REFERENCES

- Aki, K., and Richards, P.G., 1980, Quantitative Seismology: Theory and Methods, W.H. Freeman and Co., San Francisco, 932 pp
- Adriansyah, McMechan, G., 2001, AVA Analysis and Interpretation of a Carbonate Reservoir: Northwest Java Basin, Indonesia
- Hampson Russel Software, Help Documentation, Hampson Russell Software Service Ltd, Calgary, Canada.
- Ma, X-Q, 2002, Simultaneous Inversion of Pre-Stack Seismic Data for Rock Properties Using Simulated Annealing, Geophysics, 67, 1877-1885
- Maver K.G., Rasmussen, K.B., 2004, Simultaneous AVO Inversion for Accurate Prediction of Rock Properties, Offshore Technology Conference, May 2004
- Mavko G., Mukerji, T., Dvorkin, J., 1998, Rock Physics Handbook, Cambridge University Press
- Munadi, S., 2000, Aspek Fisis Seismologi Eksplorasi, Catatan Kuliah, Universitas Indonesia
- Pearl Energy Internal Report,-
- Sukmono, S., Seismik Reservoir Analysis, Lab. Of Reservoir Geophysic, Dept. of Geophysical Engineering, Institute of Technology Bandung, 2002.